MASTERARBEIT | MASTER'S THESIS

Titel | Title

Catecholaminergic enzymatic machinery in the human spinal cord and its changes after injury

verfasst von | submitted by

Anela Adilovic

angestrebter akademischer Grad | in partial fulfilment of the requirements for the degree of

Master of Science (MSc)

Wien | Vienna, 2024

Studienkennzahl lt. Studienblatt | Degree programme code as it appears on the student record sheet:	UA 066 865
Studienrichtung lt. Studienblatt | Degree programme as it appears on the student record sheet:	Masterstudium Molekulare Biologie
Betreut von | Supervisor:	Univ. Prof. Dr. Romana Höftberger

Acknowledgments

First of all, I would like to thank Univ. Prof. Dr. Romana Höftberger and Ap. Prof. DI. Dr. Karen Minassian for giving me the great opportunity to learn and grow by working on this interesting project. I am grateful for their support and all the knowledge they shared with me during the project.

I am also sincerely grateful to Dr. med. Anika Simonovska Serra, MSc for her patience in teaching me everything from scratch and for being a true mentor throughout this journey. A big thank you also goes to Ap. Prof. DI Ursula Hofstötter, PhD for her constant support.

My biggest thank you goes to my family, my parents and my brother for believing in me without a doubt. I owe my success to them. A big thank you also goes to my friends, especially Filip Milosic, who has been there for me all these years.

Contents

1. INTRODUCTION 1

1.1 Anatomy of the human spinal cord 2

1.2 Catecholamines 4

1.2.1 Alterations of the spinal catecholaminergic system following a SCI 5

1.2.2 Synthesis and metabolism of catecholamines 6

1.2.3 AADC cells in the spinal cord 7

1.2.3 DBH cells and DBH-containing axon terminals in the spinal cord 7

1.2.4 DAT in the spinal cord 8

1.2.5 Dopamine 1 (D1) and dopamine 2 (D2) receptors in the spinal cord 8

2. AIMS 9

3. Methods 9

3.1 Human tissue samples 9

3.2 Tissue processing for histological staining methods 10

3.3 Hematoxylin-Eosin and Kluver-Barrera staining 11

3.4 Immunohistochemistry (IHC) 11

3.5 Immunofluorescence (IF) 13

3.6 Western blotting 15

3.6.1 Protein extraction from human tissue 15

3.6.2 Protein determination by Lowry 16

3.6.3 Sample preparation and electrophoresis 16

3.6.4 Immunoblotting 17

3.7 Data analysis 18

4.1 TH expression in the human spinal cord – Immunohistochemistry 19

4.2 Expression of AADC in the human spinal cord 21

4.2.1. Immunohistochemistry 21

4.2.2. Immunofluorescence 26

4.2.3 Statistical analysis of AADC expression and distribution in different spinal cord gray matter regions in control and SCI cases 28

4.3 Expression of DBH in the human spinal cord 35

4.3.1 Immunohistochemistry 35

4.3.2. Immunofluorescence 36

4.4 Western blot 38

4.4.1 D1 receptor 38

4.4.2 D2 receptor 39
4.4.3 DAT 40
5. Discussion 41
5.1 TH expression in the human spinal cord 41
5.2 AADC expression in the human spinal cord 42
5.3 DBH expression in the human spinal cord 43
5.4 D1 receptor, D2 receptor and DAT in human spinal cord 44
5.5 Limitations 45
Conclusion 45
References 47
Appendix 52
Abstract 52
Zusammenfassung 53

1. INTRODUCTION

The spinal cord is part of the central nervous system (CNS) and plays an important role in motor control, reflexes and coordination and contains specialised neural networks known as central pattern generators (CPGs), which are responsible for generating the rhythmic motor patterns required for various locomotor activities[1]. These networks at the lumbar spinal level contribute to walking and can be used as a therapeutic target for individuals with leg paralysis after spinal cord injury (SCI) to restore the walking ability. The function of these neural networks depends, among others, on the presence of catecholamines in the spinal cord[2,3]. Catecholamines are a group of monoaminergic neurotransmitters including dopamine, norepinephrine (noradrenaline) and epinephrine (adrenaline)[4,5].

To date, studies on catecholamines in the spinal cord have been performed mainly in animals ranging from mammals such as mice, rats, cats and rabbits to non-human primates[6 7] . A mice model with impaired dopamine and noradrenaline biosynthesis showed severe motor dysfunctions and memory impairments suggesting the importance of catecholamines in motor control and movement regulation[8]. It has been shown that SCI affects catecholaminergic activity in animals[9–12]. By disrupting the descending pathways that transmit motor signals from the brain to the spinal cord, SCI causes a dramatic decrease or complete disappearance of catecholamines below the site of injury, resulting in severe motor impairment. Acute SCI leads to rapid depletion of catecholamine, while chronic SCI involves adaptive upregulation of local catecholamine synthesis[9–11].

Comprehensive data on catecholamines in the human spinal cord remain limited to their detection by specialized techniques such as spectrophotofluorometry and liquid chromatography in homogenized spinal cord tissue[13,14]. There were also radioligand binding and in situ hybridization studies of the adrenergic receptors in the human spinal cord[15–17]. Radioligand binding experiments in homogenised spinal cord samples showed that α2-adrenergic receptor are present in human spinal cord with a greater density in the sacral than the lumbar or thoracic spinal cord[15]. In situ hybridization identified the presence of cell bodies containing α2-adrenergic[16] and α1-adrenergic receptor[17] mRNA in cervical, thoracic, lumbar, and sacral levels of human spinal cord. The presence and distribution of catecholamines at the protein level in the spinal cord is still unknown. Moreover, the changes in expression patterns of catecholamines in the lumbar spinal cord in individuals who sustained a SCI have also not been studied yet. The limited understanding of the catecholaminergic system in the human spinal cord highlights the need for further research, which is highly relevant for pharmacological therapeutic options after spinal cord injury (SCI).

The aim of the following study was to investigate the catecholaminergic enzymatic machinery in the human spinal cord and its expression pattern after SCI. The focus of this study is the expression of aromatic L-amino acid decarboxylase (AADC), tyrosine hydroxylase (TH) and dopamine beta-hydroxylase (DBH) in human spinal cord tissue with intact central nervous system (CNS) and after sustaining a SCI by means of immunohistochemistry. Further aims were the investigation of DAT, D1, and D2 receptors through western blot analysis. Understanding the role of the catecholaminergic system and its involvement in locomotion after SCI will not only advance our knowledge of motor control but will also lead to the development of strategies that have the potential to improve walking ability after SCI.

1.1 Anatomy of the human spinal cord

The human spinal cord is a cylindrical structure consisting of 31 spinal segments, divided into eight cervical (C1-C8), twelve thoracic (Th1-Th12), five lumbar (L1-L5), five sacral (S1-S5) and one coccygeal (Cx1)[18]. Each segment of the human spinal cord corresponds to a pair of spinal nerves that emerge from the spinal cord[18,19]. The human body typically contains 31 pairs of spinal nerves with sensory and motor functions[20,21]. The spinal nerve includes two different nerve roots - dorsal (posterior) sensory roots and ventral (anterior) motor roots[21]. The exception is only the C1 spinal segment, which contains only a ventral root[21]. The dorsal nerve root transmits sensory signals from the periphery to the spinal cord, while the ventral root transmits motor signals from the spinal cord to the periphery[18,21]. The cell bodies of sensory neurons cluster together in the dorsal root, leading to the formation of a prominent enlargement called the dorsal root ganglion[20]. The spinal cord is protected by three layers of meninges, the dura mater, arachnoid mater and pia mater, which play a vital role in maintaining the elastic qualities and the stiffness of the spinal cord[18].

The spinal cord consists of white and gray matter[18,19,21]. The white matter is organised into three distinct columns: dorsal, lateral and ventral[18,21]. The white matter contains myelinated axons, which transmit signals between the brain and different spinal cord segments[19].

The gray matter has the familiar butterfly shape and is surrounded by white matter[21]. It is divided into dorsal and ventral horns and the intermediate zone, which contain different classes of neurons[18,19,21]. The dorsal horn contains interneurons that process and transmit sensory signals from the dorsal nerve roots[21]. In contrast, the ventral horn of the gray matter contains various motor neurons, primarily innervating skeletal muscles[22]. The intermediate zone is found between the dorsal and ventral horn

and contains neural circuits of interneurons and also neurons for autonomic functions[21]. The gray matter is further subdivided into Rexed's laminae I to X[18,20]. Rexed laminae I-VI occupy the dorsal horn of the spinal cord maintaining the processing of sensory signals from the dorsal roots, particularly those related to pain, touch and proprioception [19,22]. Lamina VII comprises the intermediate zone and parts of the ventral horns containing interneurons, which are connected to motoneurons and neurons in other laminae [22]. It also contains visceral motoneurons that innervate the autonomic nervous system[22]. Lamine VIII- IX are located in the ventral horn while lamina X surrounds the central canal of the spinal cord[22]. Rexed lamina IX contains the motoneurons, which are organized in columns[1,22].

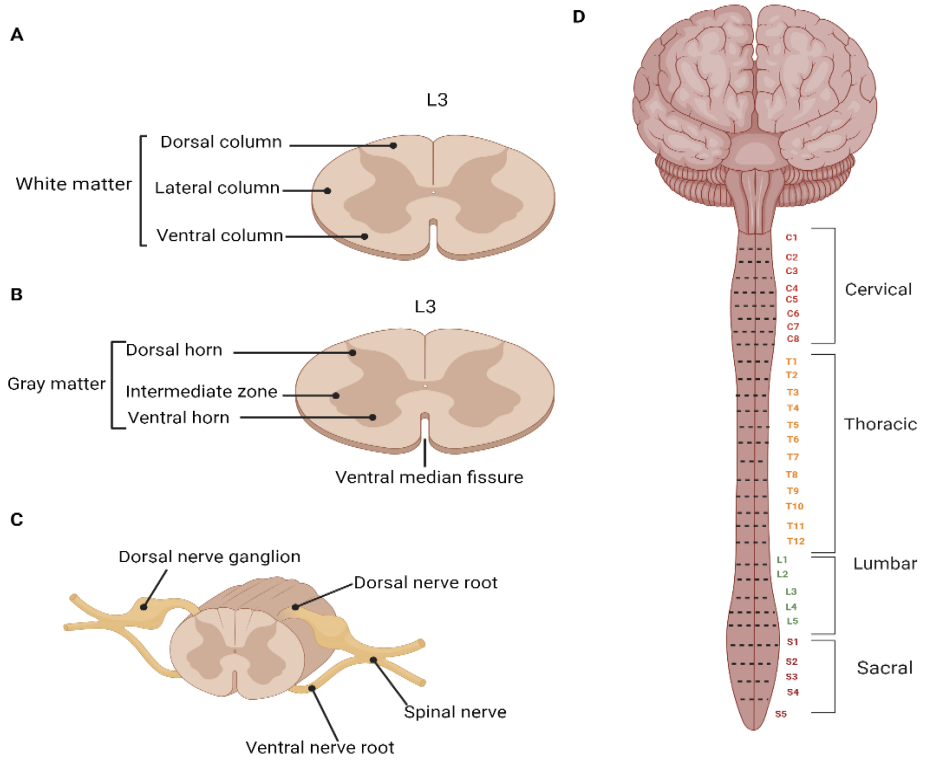

Figure 1. ***Illustration of spinal cord anatomy.*** The left side of the figure shows the organisation and distribution of white and grey matter in the spinal cord **(A-B)** and the representation of the spinal nerve with dorsal and ventral roots**(C)**. The right side of the figure shows the segmental organisation of the spinal cord **(D)**. The figure was created using BioRender.com.

1.2 Catecholamines

Catecholamines are monoaminergic neurotransmitters that play essential roles in the central and peripheral nervous systems and in the endocrine system where they function as hormones[23]. They are characterized as biogenic amines defined by catechol, a benzene ring with two hydroxyl (OH) groups in vicinal (adjacent) positions on the ring[24,25].

Catecholamines include dopamine, noradrenaline and adrenaline[23–25]. They play various physiological and psychological functions, including motor control, cognitive processes, memory processing, emotional learning and endocrine regulation[8]. Despite their similarity in structure, their production and function in the body are quite different[23]. Dopamine-producing cells are primarily located in the substantia nigra (A9 neurons), ventral tegmental area of the midbrain (A10 neurons) and the mediobasal region of the hypothalamus (A11-A14 neurons)[25]. These neurons are crucial for the regulation of motor control, memory and lerning[23,26]. The A11 neurons innervate the spinal cord[27]. In contrast to dopamine, noradrenaline is mainly produced in the locus coeruleus (A6 neurons)[28–30] and the lateral tegmental area in the brain stem (A1, A2, A5, and A7 neurons)[23]. Noradrenergic neurons are involved in cognitive processing, stress response, mood regulation, autonomic functions, pain modulation and locomotion[31–33]. Supraspinal dopaminergic of the A11 region and noradrenergic neurons of the locus coeruleus project axons into the spinal cord and release the respective neurotransmitters into the various regions of the gray matter[34]. These axons also contain the enzymes necessary to synthesize spinal catecholamines from their precursors[12,35].

Catecholamines in the spinal cord. Catecholamines have been identified in the spinal cords of rats, rabbits, oxen, pigs, cats and humans[7]. Spectrofluorometric analysis of homogenised spinal cord samples from these different species showed catecholamine concentrations similar to those found in different brain regions. In all species studied, dopamine was found in higher concentrations within the spinal cords compared to noradrenaline. The presence of adrenaline was insignificant[7]. The distribution of dopamine is well-studied in the spinal cord of rats, cats and non-human primates[36]. Immunohistochemical analysis showed the presence of dopamine in fibers and terminals in all layers of the spinal gray matter in these species, with highest expression in the dorsal horn and motoneuron clusters. The cell bodies did not exhibit immunoreactivity for dopamine[36].

In the **human** spinal cord, the presence of dopamine and noradrenaline has been demonstrated in two separate studies in different parts of the lumbar spinal cord[13,14]. In the first study, similar dopamine and noradrenaline concentrations were found in homogenized human lumbar spinal cord tissue by

means of spectrophotofluorimetry and gas chromatography and the concentration of dopamine was also similar to those reported in rat spinal cords[13].

In the second study, alterations of descending monoaminergic pathways were investigated in individuals with Parkinson's disease by using liquid chromatography and a radioenzymatic technique to measure the levels of homovanillic acid (dopamine metabolite), dopamine and noradrenaline in human lumbar spinal cord[14]. The results indicated that although spinal dopamine concentrations were similar in parkinsonian and control subjects, noradrenaline concentrations were depleted in parkinsonian patients at lumbar spinal level[14].

1.2.1 Alterations of the spinal catecholaminergic system following a SCI

The spinal cord plays an important role in motor, sensory and autonomic functions[19,21,22]. SCI leads to neuronal loss, axonal degeneration, oligodendrocyte death and demyelination, resulting in permanent sensorimotor and autonomic dysfunction[37,38]. SCI can cause paralysis below the site of injury by disrupting the descending pathways that transmit motor signals and catecholaminergic neuromodualtion from the brain to the spinal cord[10,11].

Animal studies have provided evidence suggesting that SCI also affects the concentration of catecholamines in the spinal cord[9,39]. Studies in rabbits have shown that thoracic spinal cord transection results in almost complete disappearance of noradrenaline levels below the site of injury within nine days[9]. SCI in rats led to a significant decrease in dopamine levels caudal to the site of injury one week after complete thoracic spinal cord transection[39]. However, three weeks after injury, dopamine levels were still detectable and persisted at six weeks, suggesting that the spinal cord is somehow able to produce low levels of dopamine even after injury[39].

Knowledge of the catecholaminergic system and its alternations after SCI in humans is still missing. Previous studies only provide evidence for the presence and concentration of catecholamines in the intact human spinal cord, determined by chemical methods[13,14].

1.2.2 Synthesis and metabolism of catecholamines

Catecholamine biosynthesis begins with the uptake of the amino acid tyrosine from the blood into catecholamine-producing cells[24]. Once inside, tyrosine is converted to 3,4-dihydroxyphenylalanine (L-DOPA) by the enzyme tyrosine hydroxilase (TH)[23]. L-DOPA is then decarboxylated to dopamine by the enzyme aromatic L-amino acid decarboxylase (AADC) using pyridoxal phosphate, a derivative of vitamin B6[24,40]. Once formed, dopamine is transported into synaptic vesicles by the vesicular monoamine transporter 2 (VMAT2)[34]. Dopamine can be further converted to noradrenaline by dopamine beta-hydroxylase (DBH)[40]. DBH adds a hydroxyl (-OH) group to dopamine, resulting in the formation of noradrenaline[2534].

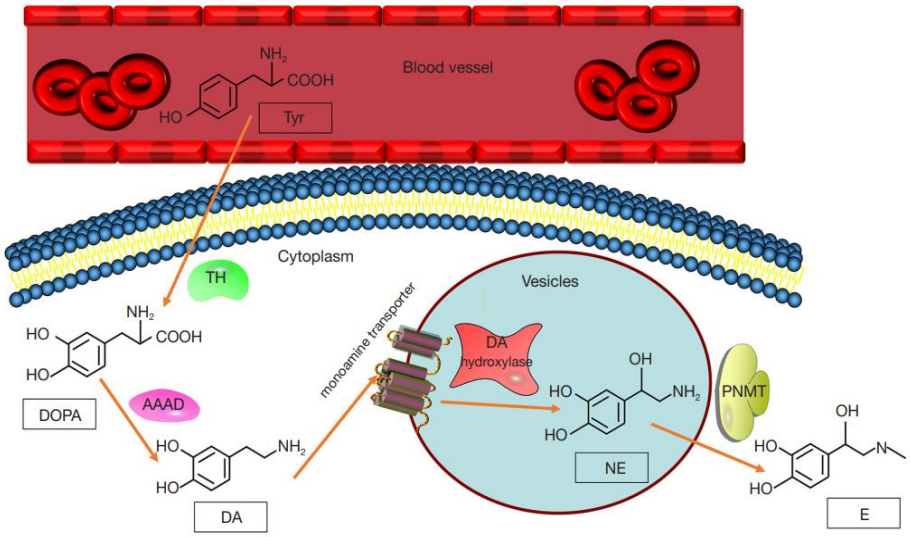

Figure 2. ***Schematic overview of catecholamine synthesis.*** *Tyr, tyrosine; DOPA, 3,4-dihydroxyphenyl alanine; TH, tyrosine hydroxylase; AAAD, aromatic amino acid decarboxylase; DA, dopamine; NE, noradrenaline; PNMT, phenylethanolamine N-methyltransferase; E, adrenaline (Liu et al., 2020).*

After synthesis and storage in specific vesicles, the catecholamines are released by exocytosis into the synaptic cleft, from where they bind to specific receptors on postsynaptic neurons[23,40]. Dopamine interacts with D1-D5 receptors, while noradrenaline and adrenaline interact with α1, α2 or β1, β2, β3 receptors on the postsynaptic neuron[23]. After transmission of signals, the catecholamines are transported back to the presynaptic neurons[40]. This process is mediated by the dopamine transporter (DAT) for dopamine and the noradrenaline transporter (NET) for dopamine[41], noradrenaline and adrenaline[23]. In presynaptic neurons, catecholamines are degraded by the enzymes catechol-O-methyltransferase (COMT) and monoamine oxidase (MAO)[40].

1.2.3 AADC cells in the spinal cord

AADC is a key enzyme in the synthesis of dopamine. It catalyzes the conversion of L-DOPA to dopamine[24,40]. Monoenzymatic AADC neurons are widely distributed in the brain and spinal cord[42]. To date, their distribution and function in the spinal cord has not been explained in detailed [43]. The AADC in the human spinal cord has not been studied.

An early study using light and electron microscopy as well as immunocytochemistry demonstrated the presence of these neurons in the Rexed lamina X of the rat spinal cord[44]. It was later shown that AADC neurons are also present in the dorsal horn, the intermediate zone and the ventral horn of rats[42,43]. The findings demonstrated that AADC neurons have different morphological characteristics throughout the spinal gray matter, suggesting that they may have different functions and roles in different physiological and pathological processes[42]. After exogenous application of L-DOPA in chronic spinal rats below the lesion, AADC positive cells became dopamine-immunopositive in the spinal cord below the lesion, whereas this effect was reduced in normal rats and sham-operated rats[43]. These results lead to the conclusion that spinal AADC cells are capable of producing dopamine from exogenous L-DOPA in response to SCI[43].

1.2.3 DBH cells and DBH-containing axon terminals in the spinal cord

DBH is an enzyme essential for the synthesis of noradrenaline from dopamine[40]. Its primary site of synthesis is the noradrenergic neuron[45]. The main sources of noradrenergic input to the spinal cord are the locus coeruleus and nucleus subcoeruleus in the pons [46].

In rats, DBH has been found in the axon terminals of noradrenergic fibers throughout the spinal gray matter at all levels of the spinal cord[47]. These findings were confirmed by studies in non-human primates where DBH-positive noradrenergic fibers were mainly observed in the ventral horn around the large motor neurons, in the marginal layer of the dorsal horn, around the central canal and in laminae IV-VI[46].

In chronic spinal rats, the presence of DBH-positive fibers and terminals in the intermediolateral cell column (ILC) was significantly reduced caudal to transection, compared to control rats or segments rostral to the transection, but DBH was upregulated in the cytoplasm of neurons in the dorsal horn (laminae IV and VI) and in the intermediate zone of the gray matter in spinal segments below the

lesion[40]. These results were confirmed in a subsequent study that examined the colocalization of DBH and growth-associated protein-43 in rats before and after spinal cord transection[48]. Taken together, these results demonstrate that the spinal cord undergoes a reorganization of synaptic plasticity after SCI.

1.2.4 DAT in the spinal cord

DAT is a plasma membrane protein that is expressed in dopaminergic neurons[49]. It is responsible for the reuptake of dopamine from the synaptic cleft into the presynaptic neuron[50]. In the spinal cord of non-human primates, mice and rats, DAT was absent in the A11 nerve terminals, the main source of dopaminergic spinal innervation[39,51,52]. The molecular mechanism of dopamine reuptake in the spinal cord remains unclear and has not yet been investigated in the human spinal cord[51,52].

1.2.5 Dopamine 1 (D1) and dopamine 2 (D2) receptors in the spinal cord

Dopamine acts via G-coupled receptors classified as D1-like (D1 and D5) and D2-like (D2, D3, and D4) receptors[53]. D1-like receptors are located on non-dopaminergic neurons and have excitatory effects. D2 receptors are located on non-dopaminergic neurons with inhibitory effects by inhibiting cAMP pathway as well as on dopaminergic neurons where they act as autorecepetors to inhibit dopamine release[54]. A quantitative real-time polymerase chain reaction (PCR) and in situ hybridization technique demonstrated the presence of all five receptors in the lumbar spinal cord of mice, with predominant D2 receptor expression and similar distribution across all laminae of the spinal gray matter[53]. A study with autoradiography in rats showed different spinal distributions of D1 and D2 receptors[55]. D1 receptors were highly concentrated in the ventral horn, while D2 receptors were hardly detectable in this region. Conversely, the substantia gelatinosa showed a high density of D2 receptors, but very low amounts of D1 receptors. In addition, D1 receptors were more present in the cervical and lumbosacral segments than in the thoracic segments[55]. The different expression and distribution of dopamine receptors was also confirmed in the spinal cord of non-human primates[51]. In situ hybridization showed that the mRNA of the D1 receptor was not present in the spinal cord of non-human primates, whereas the mRNA of the D2 receptor was mainly expressed in the dorsal horn of the spinal cord[51]. Dopamine receptors have not been studied in the human spinal cord.

2. AIMS

This study hypothesises that SCI is associated with changes in the expression of the catecholamine enzymatic machinery (TH, AADC, DBH) in the human lumbar spinal cord. To test these hypotheses, the following aims were proposed:

- To provide a spatial distribution of TH, DBH and AADC in different regions of the human lumbar spinal cord by immunohistochemistry in formalin-fixed, paraffin-embedded autopsy tissue.
- To compare the expression of TH, DBH and AADC in intact spinal cord tissue and after SCI.
- To extend the analysis of the dopaminergic system of the human spinal cord, further aims were to determine the expression of DAT, D1 and D2 receptors in intact human lumbar spinal cord tissue by Western blot analysis.

3. Methods

3.1 Human tissue samples

Human spinal cord and brain tissue samples were obtained from the archival autopsy material of the Division of Neuropathology and Neurochemistry, Department of Neurology, Medical University of Vienna. All parts of the performed work were approved by the ethics committee of the Medical University of Vienna (EK. Nr.: 1123/15 and 1636/2019) ensuring compliance with ethical guidelines and standards.

This study was performed on four post-mortem human intact spinal cord samples and three post-mortem human spinal cord samples with sustained SCI. Comprehensive medical records of the subjects used in this study including age, cause of death, type of injury, cause of injury, lesion site, and time post-injury were collected and are listed in Tables 1 and 2.

Human brain tissues including substantia nigra, pons and hippocampus were used as positive controls. The tissues for the validation procedures were selected based on the literature that reported the expression of TH, AADC, DBH, D1 and D2 receptors and DAT in the specific brain areas[56–61]. According to the literature, the substantia nigra was used for the validation of TH and AADC

immunohistochemical analysis, while the pons was used for the validation of DBH (Table 4). Validation of Western blot analysis of the D1 receptor and DAT was performed on substantia nigra, while the hippocampus was used for validation of D2 receptor.

Table 1. Subjects with spinal cord injury (SCI)

Subjects	Gender	Age at death	Cause of death	Completeness of SCI	Cause of injury	Lesion level	Time post injury
1	male	46	respiratory insufficiency	complete	fall accident	C4-C7	4 days
2	female	34	respiratory insufficiency	complete	Polytrauma	lower cervical, upper thoracic	180 days
3	male	58	cardiovascular failure	complete	fall accident	C8	413 days

Table 2. Control subjects with intact spinal cord and no neurological diseases

Subjects	Gender	Age at death	Cause of death
1	male	61	cardiovascular failure
2	female	15	respiratory insufficiency
3	male	66	Peritonitis
4	male	79	cardiovascular failure

3.2 Tissue processing for histological staining methods

Human autopsies were formalin-fixed and paraffin-embedded using a Tissue-Tek TEC™ embedding device. The paraffin-embedded tissue sections were cut at 3 µm thickness on a rotatory microtome (Thermo Scientific, Shandon Finesse ME+), and attached to adhesive glass microscope slides (Star Frost 76x26 mm, Knittel Glas GmbH, Germany).

The tissue sections were then incubated at 70°C for 30-60 minutes. After cooling at room temperature, the tissue sections were stained or stored at -30°C until further use.

3.3 Hematoxylin-Eosin and Kluver-Barrera staining

To characterize the morphology and anatomy of the human tissue samples, Hematoxylin-Eosin (HE) and Kluver-Barrera staining were performed. For the HE staining, tissue sections were deparaffinized in xylene (Thermo Fischer Scientific ™, Cat. #447240010) two times for ten minutes, hydrated three times in 96%, one time in 80%, 70%, and 50% ethanol, and one time in distilled water. The sections were then incubated in Mayer´s Hemalaun solution (Merck, Cat. #109249) for four minutes, three times washed in cold tap water, immersed five to ten times in HCL ethanol, and washed in warm tap water. The tissue sections were then stained in Eosin (ROT, Cat. #3137.2) for a duration of three minutes. The tissue sections were rinsed with cold tap water and dehydrated through ascending ethanol series (one time in 50%, one time in 70%, and three times in 96%) and n-butyl acetate (Merck, Cat. #109652). The slides were then coverslipped with CONSUL-MOUNT mounting medium (Thermo Scientific ™, Cat. #9990441).

For the Kluver-Barrera staining, tissue sections were deparaffinized two times in xylene, hydrated three times in 96% ethanol, and stained in 0,1%, Luxol Fast Blue (RAL DIAGNOSTICS, Cat #1328-51-4) at 56°C-60°C, overnight. On the next day tissue sections were rinsed with 96% ethanol and distilled water and incubated in 0,1% aqueous lithium carbonate solution for three minutes. Afterwards, the differentiation was performed by immersion in 70% ethanol, followed by washing in distilled water. For characterisation of cellular nuclei, the slides were incubated in Kernechtrot staining solution (Morphisto, Cat. #10264) for 15-20 minutes. Slides were then washed in distilled water, dehydrated once in 50%, once in 70%, three times in 96% ethanol, and in n-butyl acetate. Finally, the slides were coverslipped with a CONSUL-MOUNT mounting medium.

3.4 Immunohistochemistry (IHC)

Deparaffinization and hydration of formalin-fixed paraffin-embedded human spinal cord tissue were performed by immersing the tissue sections in xylene two times for ten minutes, passing them through ethanol solutions of decreasing concentration (three times in 96%, and one time in 80%, 70%, and 50% ethanol), and washing in distilled water. In order to reduce the unspecific binding of the secondary antibody detection system, the endogenous biotin activity was blocked by incubation of tissue sections in 3% hydrogen peroxide in methanol for ten minutes, followed by washing in tap water. Antigenic epitopes masked by formalin fixation were retrieved by incubation of the tissue section in an

appropriate buffer heated to 95°C in a PT Linker (Agilent Technologies, Inc.) for approximately 30 minutes. After heat-induced antigen retrieval and washing three times in Tris-buffered saline solution (TBS), the tissue sections were encircled with a hydrophobic IHC pen (Cat. # N71310-N) to create hydrophobic barriers that ensure that the blocking and antibody solutions cover the tissue sections properly after putting them in a wet chamber. A wet chamber is used to prevent drying of the slides during incubation with primary and secondary antibodies. Unspecific binding sites were blocked with EnVision FLEX Antibody Diluent (Dako, Cat. #K8006) or with 10% normal donkey anti-goat serum dissolved in TBS, depending on the primary antibody that was used. In this study, we performed IHC stainings for DBH, TH and AADC (Table 3). The blocking step in IHC staining for DBH and TH was performed by incubation of the tissue sections in EnVision FLEX Antibody Diluent for ten minutes at room temperature (RT). Afterwards, DBH and TH primary antibodies were diluted in the same solution used for blocking and incubated overnight at 4°C. In the case of AADC, unspecific binding sites were blocked with 10% normal donkey anti-goat serum in TBS for 1h at RT, followed by overnight incubation with AADC primary antibody in 1% donkey anti-goat serum in TBS at 4°C.

On the next day, all tissue sections were washed three times in TBS. The tissue sections that were incubated overnight with TH and DBH primary antibodies were treated with peroxidase-linked goat anti-rabbit/mouse secondary antibody (EnVision Detection System, Dako, Cat. #K5007) at RT for 25 minutes, while the AADC tissue sections were treated with donkey anti-goat HRP diluted 1:500 in 1% donkey anti-goat serum in TBS for 30 minutes. Dilutions are summarized in Table 3. After three washes in TBS, the staining was developed with a 3,3'-diaminobenzidine (DAB) solution. The solution was prepared according to the manufacturer's instructions (Dako, Cat. #K3468) and was pipetted onto the tissue twice for five minutes.

Next, the tissue sections were washed in tap water and counterstained with haematoxylin solution for 30 seconds. After the counterstaining, the sections were immersed in tap water and in HCL alcohol for 10 seconds. Then, the slides were rinsed and washed in warm tap water for three minutes and dehydrated by immersion in 70% and 3x 96% ethanol solutions. Finally, the tissue sections were immersed twice in n-butyl acetate and the slides were mounted with CONSUL-MOUNT mounting medium. The stained tissue sections were analyzed and scanned using a light microscope (Olympus, BH-2) and the NanoZoomer 2.0-HT slide scanner system (Hamamatsu Photonics).

3.5 Immunofluorescence (IF)

The double immunofluorescence method was used to analyse the co-expression patterns of DBH or AADC with the non-phosphorylated neurofilament protein SMI32. As described above, deparaffinization, rehydration, blocking of endogenous biotin with 3% hydrogen peroxide in methanol and antigen retrieval was performed. Nonspecific binding was inhibited by incubation of the tissue sections in appropriate blocking buffers. The fluorophores used in the IF experiments were diluted to achieve an optimal signal-to-noise ratio (Table 5).

For a double-immunofluorescence staining with DBH and SMI32, the blocking step was performed with 10% NGS (Normal goat serum, Gibco™, Cat. #16210064) dissolved in TBS for 1h at RT. The primary antibody against DBH was diluted 1:50 in 1% NGS in TBS and was incubated at 4°C overnight. The following day, DBH was briefly washed out with TBS and the primary antibody SMI32 diluted 1:500 in 1% NGS in TBS was incubated at 4°C overnight. On the third day, the tissue sections were washed three times in TBS to ensure the removal of any residual substances. Subsequently, the sections were incubated with fluorophore-conjugated secondary antibodies Alexa Fluor 488 (AF488) goat anti rabbit IgG targeting DBH and Cy3 goat anti mouse IgG targeting SMI32 in the dark for 2h at RT.

The double immunofluorescence staining of AADC and SMI32 was performed using 10% normal donkey serum as a blocking solution, dissolved in TBS, and incubated at RT for a duration of 1h. Following the blocking step, the tissue sections were subjected to overnight incubation with AADC primary antibody diluted 1:50 in 1% normal donkey serum in TBS at 4°C. On the second day, AADC was briefly washed out with TBS and the primary antibody SMI32 was applied with a dilution of 1:500 in 1% normal donkey serum in TBS and incubated overnight at 4°C. The next day, the sections were incubated with a biotinylated secondary antibody donkey anti mouse IgG diluted 1:500 in 1% normal donkey serum for 30min at RT. Afterwards, the slides were washed with TBS and were incubated with fluorophore-conjugated secondary antibodies dissolved in 1% normal donkey serum in TBS at RT for 2h in the dark. Specifically, Alexa Fluor 488 (AF488) donkey anti goat IgG was used for AADC and Cy3 Streptavidin for SMI32, which was previously incubated with a biotinylated secondary antibody donkey anti mouse IgG, as described above.

After incubation with primary and fluorophore-conjugated secondary antibodies, the nuclei were stained with DAPI (4',6-diamidino-2-phenylindole, Invitrogen™, Cat. #D1306) in TBS for five minutes. Next, the tissue sections were rinsed in TBS and distilled water, and were cover slipped with Aqua Poly/mount, (Polysciences, Cat. #18606) a water-soluble, aqueous mounting medium for preserving

the stained tissue. The slides were kept in the dark at 4°C and after drying, the stained tissue was imaged utilizing a fluorescence microscope (Olympus BX63) and the slide scanner Vectra Polaris.

Table 3. List of primary antibodies used in IHC and IF experiments.

Antibody	Clone	Host	Dilution factor		Antigen retrieval	Company	Catalog number
			IHC	IF			
DBH (Dopamine beta-hydroxylase)	mAb	Rabbit	1:250	1:50	pH 6	Abcam	AB96615
TH (Tyrosine hydroxylase)	mAb	Mouse	1:50	-	pH 6	Leica Biosystems Newcastle	NCL-TH
AADC (Aromatic l-amino acid decarboxylase)	pAb	Goat	1:100	1:50	pH 9	Invitrogen	PA5-47512
SMI32 (Non-phosphorylated neurofilament protein)	mAb	Mouse	-	1:500	pH 6	BioLegend	801701

mAB, monoclonal antibody; pAb, polyclonal antibody; -, staining is not performed; pH6, antigen retrieval of tissue sections in citrate buffer of pH 6.0 (EnVision FLEX Target Retrieval Solution low pH, Dako, Cat. #K8005); pH 9, antigen retrieval of tissue sections in EDTA buffer of pH 9.0 (EnVision FLEX Target Retrieval Solution high pH, Dako, Cat. #K8000/K8002).

Table 4. List of positive control brain tissue used in IHC and IF stainings.

Antibody	Positive control
DBH	Pons
TH	Substantia nigra
AADC	Substantia nigra

Table 5. List of fluorophores and their respective dilutions used in IF experiments.

Fluorochrome	Color	Absorption(nm)/Emission(nm)	Dilution/ Concentration	Company	Catalog Number
AF488 goat anti-rabbit IgG	green	495/519	1:800	Invitrogen	A11034
Cy3 goat anti-mouse IgG	orange	550/570	1:1000	Jackson Immuno Research	163462
AF488 donkey anti-goat IgG	green	495/519	1:800	Abcam	ab150129
Cy3 streptavidin	orange	550/570	1:1000	Jackson Immuno Research	164550
Dapi	ultraviolet	358/465	1ug/ml in TBS, 1:1000	Invitrogen	D1306

3.6 Western blotting

3.6.1 Protein extraction from human tissue

Human spinal cord, substantia nigra and hippocampus tissue were frozen directly after harvesting using liquid nitrogen and were stored at -80°C until further use. The hippocampus and substantia nigra were used as positive controls for the antibodies. Then, the tissue samples were thawed on ice, weighed, cut into small pieces and transferred into a homogenization tube. The measured tissue weight was multiplied by four and an equal amount of 1X RIPA buffer (Radio-immunoprecipitation assay buffer, Millipore, Cat. #20188) and PIC (Protease inhibitor cocktail, Sigma-Aldrich, Cat. #P8340-5ML) at 1:100 dilution were added to the homogenization tube. The tissue was then homogenized using a tissue grinder and transferred into an Eppendorf tube. All these steps were performed on ice. Before centrifugation, the tissue-homogenized lysate was incubated on ice for 10 min and then exposed to UV light two times for 10 seconds. Centrifugation was performed at a speed of 10000 rpm at 4°C for 10 min and the supernatant containing the proteins was collected and stored at -80°C until further use.

3.6.2 Protein determination by Lowry

The protein concentration was determined by using the protein determination method by Lowry[62]. First, we prepared and combined solutions A, B, C and E in the following manner:

Solution A (0,1 M NaOH)

Solution B (2% Na_2CO_3 in 50 ml of solution A)

Solution C (0,5% $CuSO_4$ and 1% $Na_3C_6H_5O_7$)

Solution D (1 ml of solution C in 50 ml of solution B)

Solution E (Folin- Ciocalteus reagent diluted with an equal volume of distilled water).

One blank tube was filled with 500 µl of distilled water to measure the absorbance caused by non-protein components in the reagents and solutions ensuring the accuracy of the subsequent protein concentration measurement. Two probes per tissue were used for a double determination process. The tissue probes were filled with 20 µl of tissue sample and 480 µl of distilled water. Following this, 5 ml of solution D was added into both the blank and probes, vortexed, and incubated for 10 minutes at RT. Subsequently, 500 µl of solution E was added to blank and probes, vortexed, and incubated at RT for a duration of 1h. After incubation, the small aliquot of protein-reagents mixture was transferred to measuring cuvettes, and the absorbance of the tissue sample was measured at a wavelength of 760 nm, using a Hitachi U-2910 spectrophotometer.

3.6.3 Sample preparation and electrophoresis

According to the measured protein concentration, the volume of the protein extract corresponding to 30-60 µg was mixed with 1x RIPA buffer and sample buffer (GenScript, Cat. #MBO1015). A total of 20µl of the sample was boiled at 95°C for five minutes and loaded onto mini polyacrylamide gels with gradient concentration ranging from 4-20% (SurePage™,Cat. #M00655). For correct protein size determination, 5µl of PageRuler™ Plus Prestained Protein Ladder (ThermoScientific™ Cat. #26619) were loaded as well. The electrophoresis was run at 100 V for 1h and 20 minutes using MOPS as a running buffer, prepared according to the manufacturer's instructions (Biozol, Cat. #M00138).

3.6.4 Immunoblotting

Blotting onto nitrocellulose membranes (Millipore, Cat. #IPVH304F0) was performed on ice with a wet transfer at 100 V for 1h. The transfer sandwich was prepared by placing the macroporous sponge on the black side of the mini wet transfer cassette followed by four filter papers and polyacrylamide gel. Subsequently, the membrane was first immersed in methanol for a few seconds, then in distilled water for five minutes and then placed directly on a gel. The transfer sandwich was completed by placing another four filter papers and a second macroporous sponge on top of this layered arrangement. Finally, the assembled transfer sandwich was inserted into a wet transfer apparatus filled with a transfer buffer. To ensure the controlled and optimized transfer environment the magnetic fish was positioned under the transfer cassette, the transfer apparatus was then placed on an ice-cooled stirrer and subjected to a controlled electrical potential of 100 V for 1h. After transfer, the membranes were briefly rinsed with TBST and blocked in Every Blot Blocking Buffer (BIO-RAD, Cat. #12010020) with gentle shaking for 10 minutes at RT. Following the blocking step, the membranes were incubated with a primary antibody at 4°C overnight on a shaking device (Table 6). On the next day, membranes were incubated with a goat anti-rabbit IgG secondary antibody (BIO-RAD, Cat. #1706515) conjugated to horse-radish peroxidase (HRP) at a dilution of 1:3500 for 1 h at RT. Primary and secondary antibodies were diluted in the solution used for blocking, and each incubation included gently shaking on a shaker to ensure uniform and optimal binding of antibodies. After each incubation with antibodies, the membranes were washed in TBST three times for five minutes. Protein visualization was performed using the Clarity Max^{TM}Western ECL Substrate according to the manufacturer's instructions (BIO-RAD, Cat. #1705062). Detection was performed using a Fusion EDGE FX6 imaging system.

Table 6. Primary antibodies used for Western blotting.

Primary antibody	Host	Dilution	Molecular weight (kDa)	Company	Catalog number
Dopamine 1 receptor	Rabbit	1:750	**49,293** suggested by UniProt	Invitrogen	702593
Dopamine 2 receptor	Rabbit	1:1000	**50.619** suggested by UniProt and the company	Millipore	AB5084P
Dopamine Transporter	Rabbit	1:1000	**88**	Millipore	AB1766

			suggested by company		

3.7 Data analysis

The immunopositivity of TH was described qualitatively. The western blot data for DAT, D1 and D2 as well as the immunohistochemical staining for DBH were performed on only one case each, and the expression was described qualitatively.

The expression of AADC was assessed semi-quantitatively with the software QuPath, an open-source software for digital pathology[63]. The spinal gray matter was divided into the dorsal horn, the intermediate zone and the ventral horn. Substantia gelatinosa corresponding to lamina II in the dorsal horn, the motoneurons of lamina IX in the ventral horn and the central canal corresponding to lamina X were analysed separately. The semi-quantitative scoring system included +++ for strong expression, ++ for intermediate expression, + for weak expression and – for no expression.

Statistical analysis was performed using IBM SPSS Statistics 28.0.1.1 for Windows (IBM Corporation, Armonk, NY, USA). To explore the potential associations between CNS state (control, and SCI) and AADC expression levels, we conducted separate $\chi 2$-tests of independence or Fisher exact tests for each spinal cord area examined as well as the expression within the membrane and cell bodies. The strength of associations was indicated by Cramer's V. α-errors of $P < .05$ were considered significant. Adjusted residuals with absolute values > 2 were considered to indicate significant deviations from independence.

4. Results

4.1 TH expression in the human spinal cord – Immunohistochemistry

The expression pattern of TH was investigated in human spinal cord tissue from subjects with complete spinal cord transection and controls with intact spinal cords. The specificity of the antibody used against TH was tested and confirmed on human substantia nigra tissue that served as a positive control (**Figure 3**).

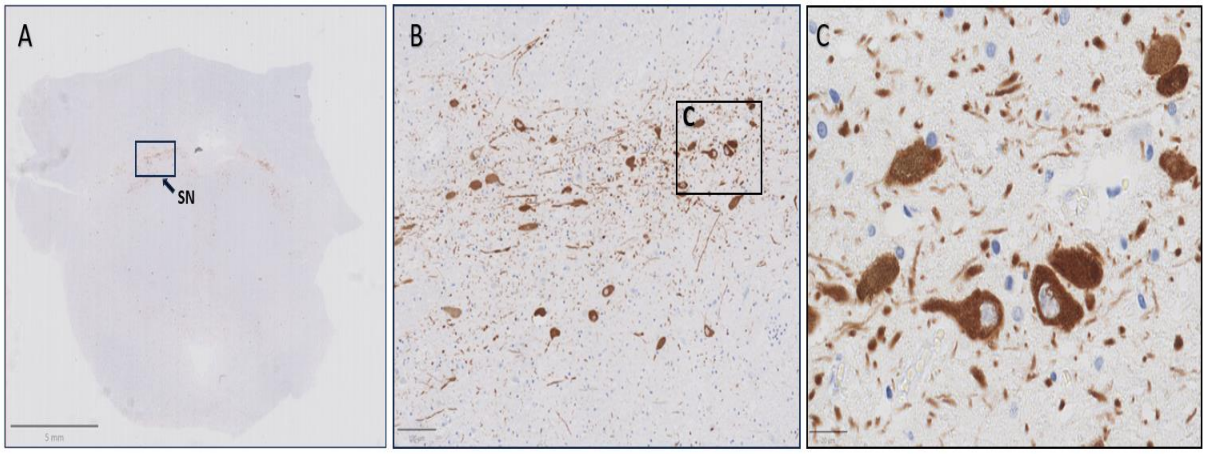

Figure 3. A *Cross-section of the human midbrain stained with an antibody against TH. The box in A highlights the substantia nigra (SN).* ***B*** *Close-up view of the SN demonstrating positive cytoplasmatic neuronal staining of TH.* ***C*** *TH-positive neurons within the SN presented at higher magnification. Scale bars indicate 5 mm, 100 µm, and 20 µm for* ***A****,* ***B****, and* ***C*** *respectively.*

In the control subjects, a weak TH expression was observed predominantly in axonal terminals of putative supraspinal origin, in the dorsal horn, the intermediate zone and in the ventral horn of the lumbar spinal gray matter **(Figures 4 and 5)**. Notably, no immunoreactivity was detected in neuronal cell bodies in the spinal cord tissue of either group. TH was not expressed in subjects 2 and 3 subjects with chronic SCI, whereas in subject 1 with acute SCI faint TH expression was detected in axonal terminals in the dorsal horn and the intermediate zone (data not shown).

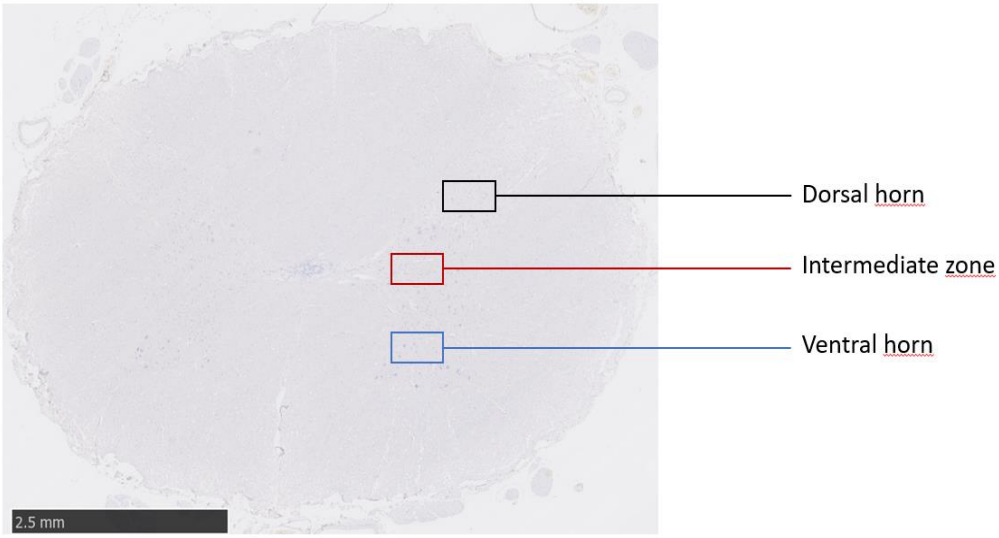

Figure 4. Cross-section of lumbar segment stained with TH-antibody. *Specific areas of the spinal gray matter corresponding to the dorsal horn, intermediate zone, and ventral horn are marked in black, red, and blue, respectively. Scale bar 2.5 mm.*

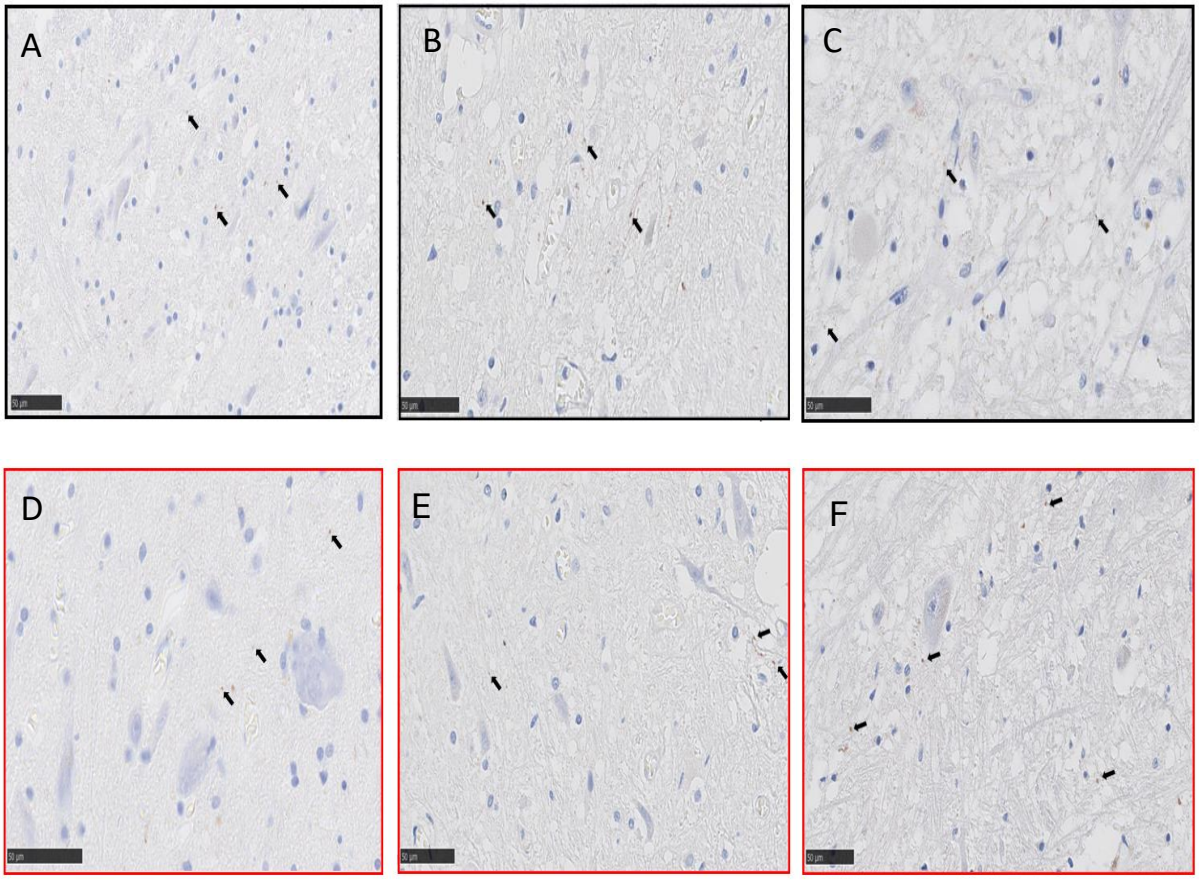

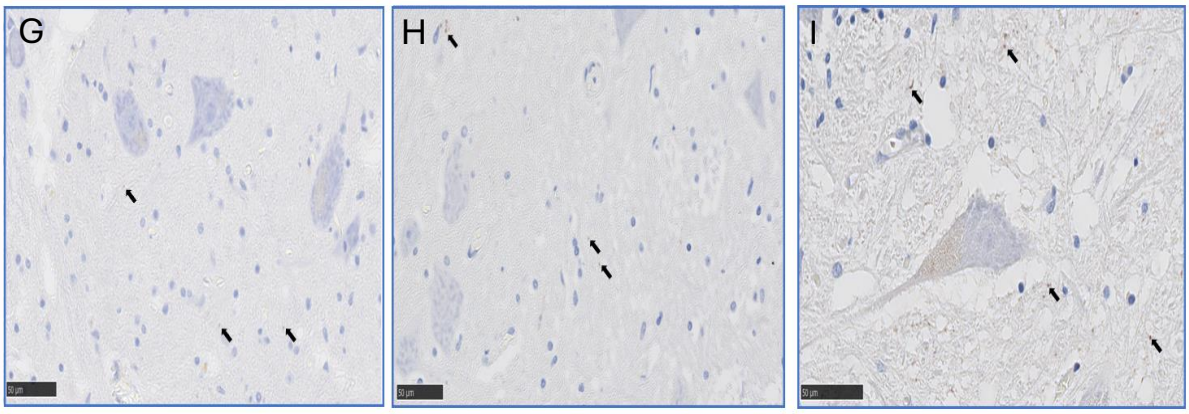

Figure 5. TH expression in spinal cord tissue from subjects with intact spinal cord.
A-C *TH expression patterns in the dorsal horn in the spinal cord tissue from subjects 1, 2 and 3 respectively.* ***D-F*** *TH expression patterns in the intermediate zone in the spinal cord tissue from subjects 1, 2 and 3 respectively.* ***G-I*** *TH expression patterns in the ventral horn of spinal cord tissue from subjects 1, 2 and 3 respectively. Arrows indicate TH immunoreactivity observed at axonal terminals of likely supraspinal origin. Scale bars 50 µm.*

4.2 Expression of AADC in the human spinal cord

4.2.1. Immunohistochemistry

The AADC antibody was first validated in the human midbrain, showing strong immunopositivity of neurons throughout the substantia nigra (**Figure 6**).

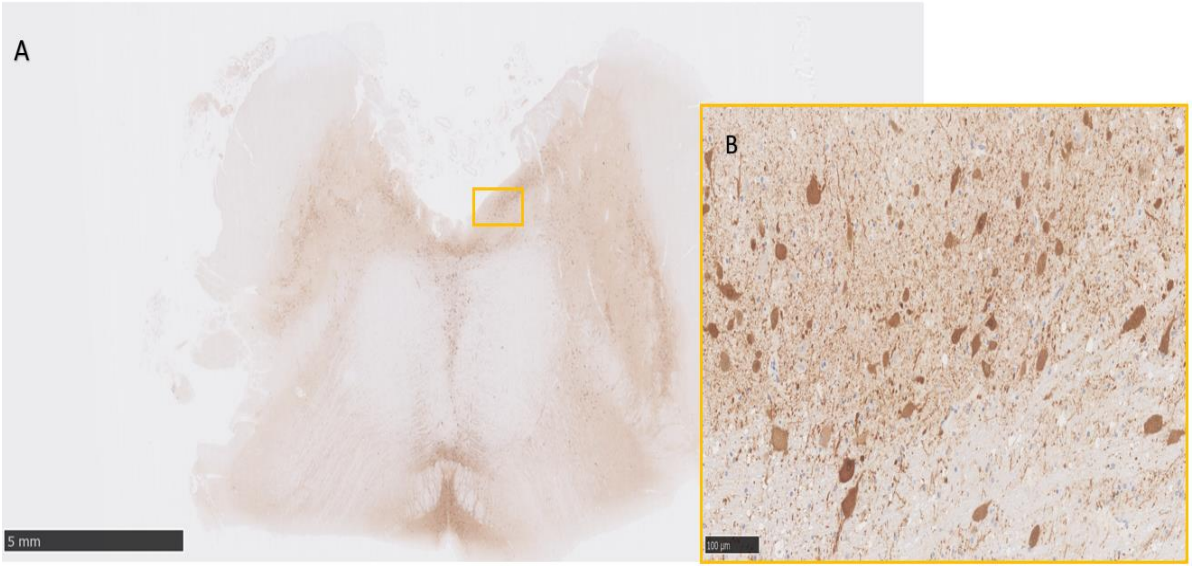

***Figure 6. A** Human midbrain stained with AADC with the box highlighting the substantia nigra (SN) (scale bar 5 mm). **B** Higher magnification of SN showing AADC immunoreactivity in neuronal processes and in the cytoplasm of neurons (scale bar 100 µm).*

After confirming the specificity of the antibody, we investigated the AADC expression in the spinal cord of subjects with sustained SCI and control subjects with intact spinal cord. In the control group, AADC was detected predominantly on the membrane of neurons as well as in neuronal processes. Additionally, AADC was also found in blood vessels. The expression pattern was very similar within the control group and was characterized by a bilateral symmetry in the dorsal horn, the intermediate zone and in the ventral horn **(Figures 7 and 8)**. AADC was also observed on membranes of motoneurons **(Figure 9)**. A small number of neurons also demonstrated a stronger cytoplasmic staining, mainly in Clarke's column **(Figure 10)**. In subjects with chronic SCI, the AADC immunopositivity was detected in the cytoplasm of neurons in the dorsal, intermediate and ventral horn. Some immunoreactivity was still observed in neuronal processes and on neuronal membranes, but to a lesser extent compared to the control group. In subject 1 with acute SCI, the expression pattern of AADC was very similar to the control group **(Figure 11).**

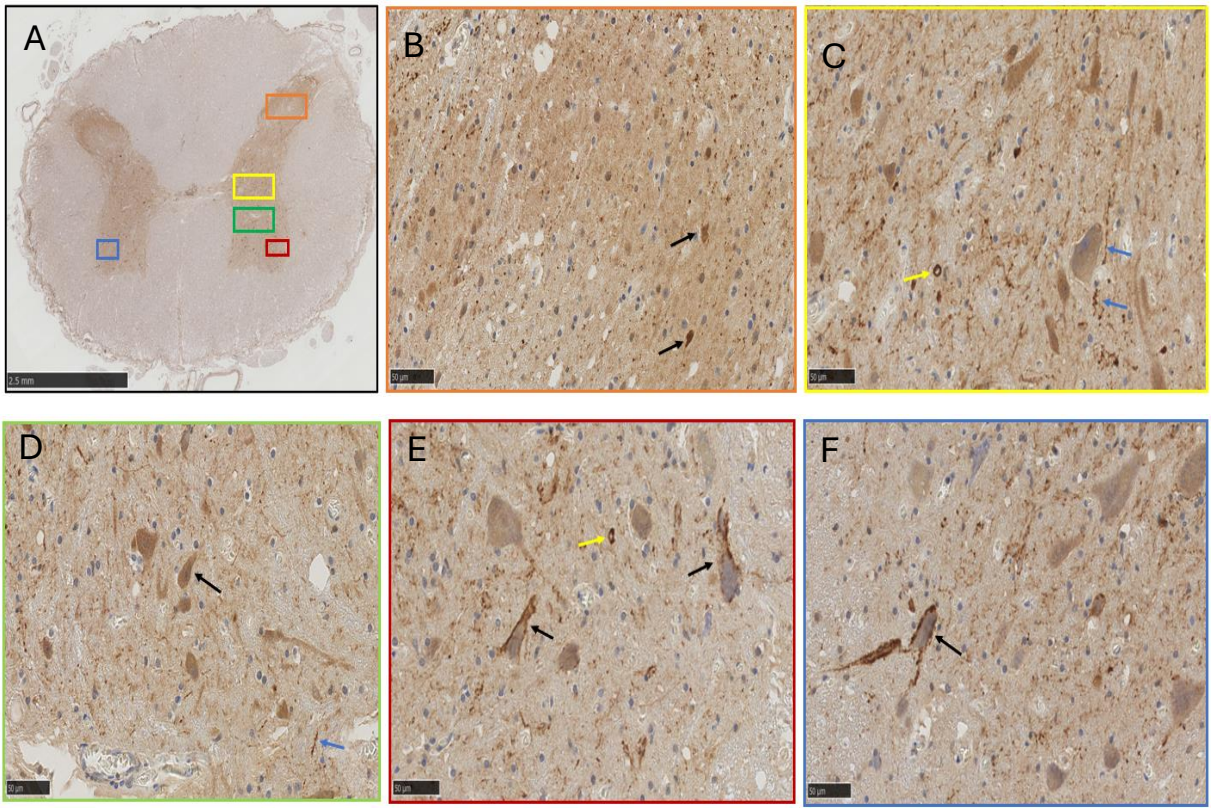

***Figure 7. A** AADC staining of a control subject 1, L1 segment with boxes highlighting the substantia gelatinosa in orange, the intermediate zone in yellow, the dorsomedial ventral horn in green and ventrolateral zones in blue and red (scale bar 2.5 mm). **B** Substantia gelatinosa with black arrows*

marking positive neurons. ***C*** *Intermediate zone with blue arrows indicating AADC expression on neuronal processes and a yellow arrow pointing to AADC localization within blood vessels.* ***D*** *Faint cytoplasmatic staining of AADC in neurons of the dorsomedial ventral horn.* ***E*** *-* ***F*** *Strong membranous expression of AADC in ventrolateral neurons (B-F scale bars 50 µm).*

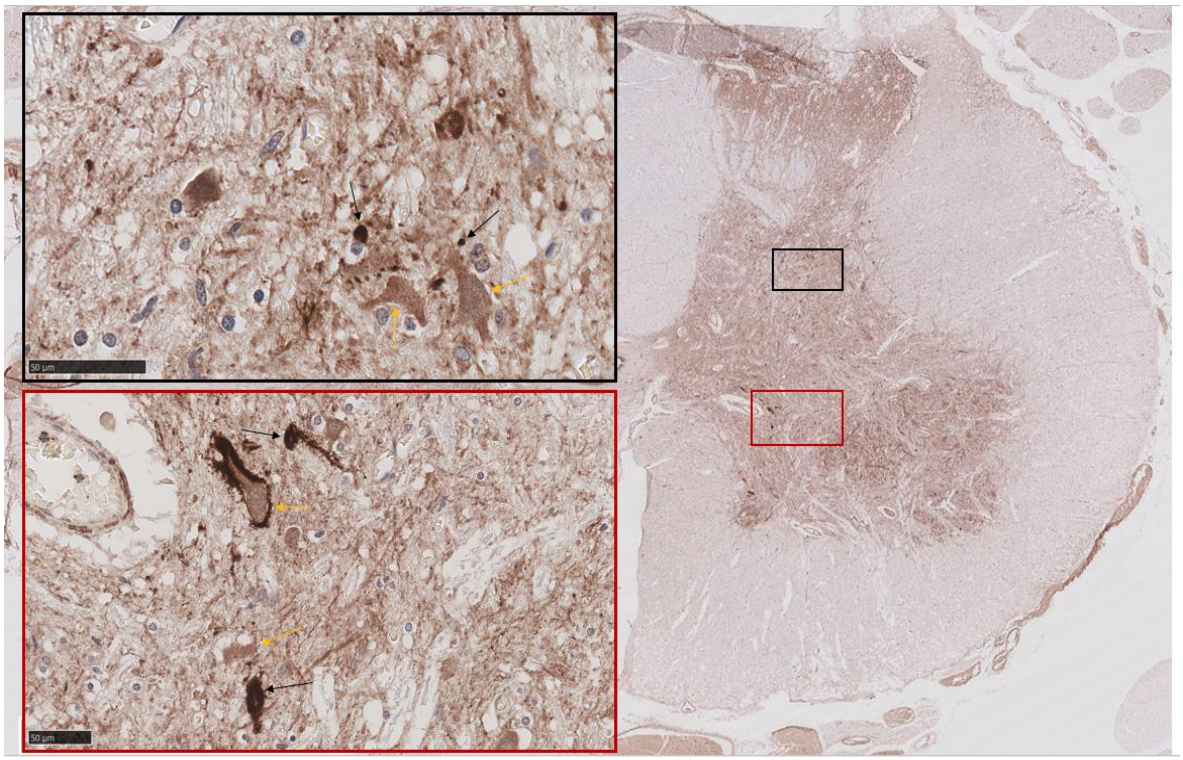

Figure 8. *L4 segment of control subject 3. Highlighted regions show neurons with strong expression on neuronal membranes and neuronal processes (black arrows). Faint AADC staining in the cytoplasm of neurons (yellow arrows).*

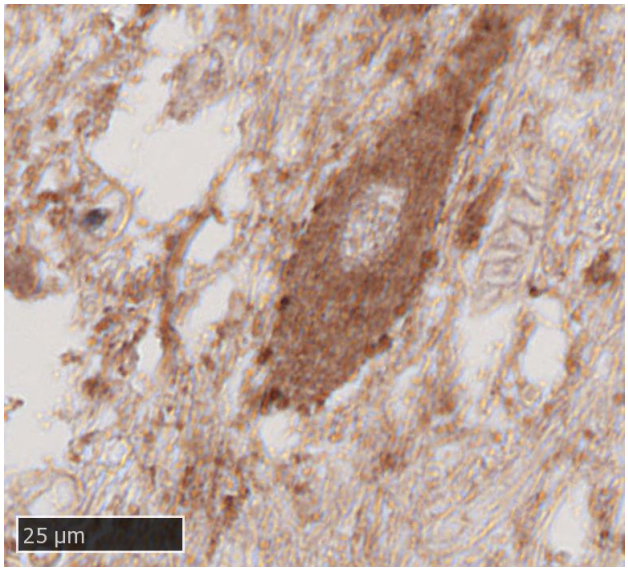

Figure 9. *Motoneuron in lamina IX with positive AADC immunoreactivity on the membrane and faint cytoplasmatic staining in control subject 4 (scale bar 25 µm).*

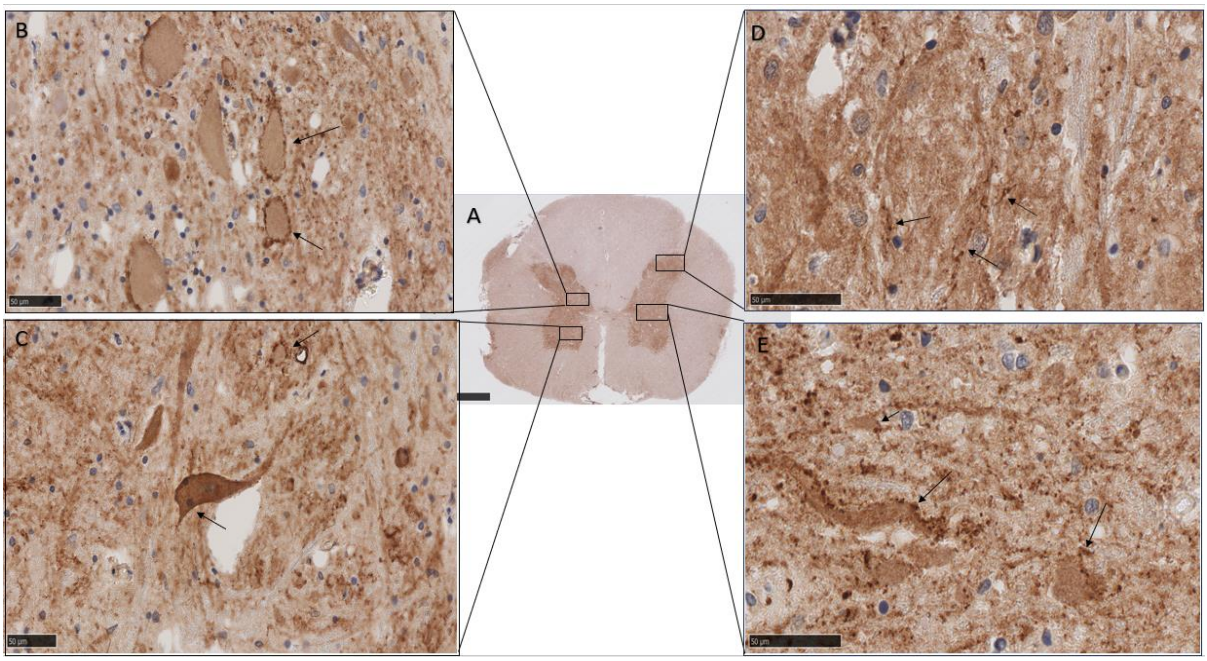

Figure 10. ***A*** *AADC staining of control subject 2, L1 segment.* ***B-E*** *Highlighted areas of the spinal gray matter at higher magnification. Arrows indicate AADC-positive neurons with strong expression on the membrane and on neuronal processes (scale bars 50 µm).*

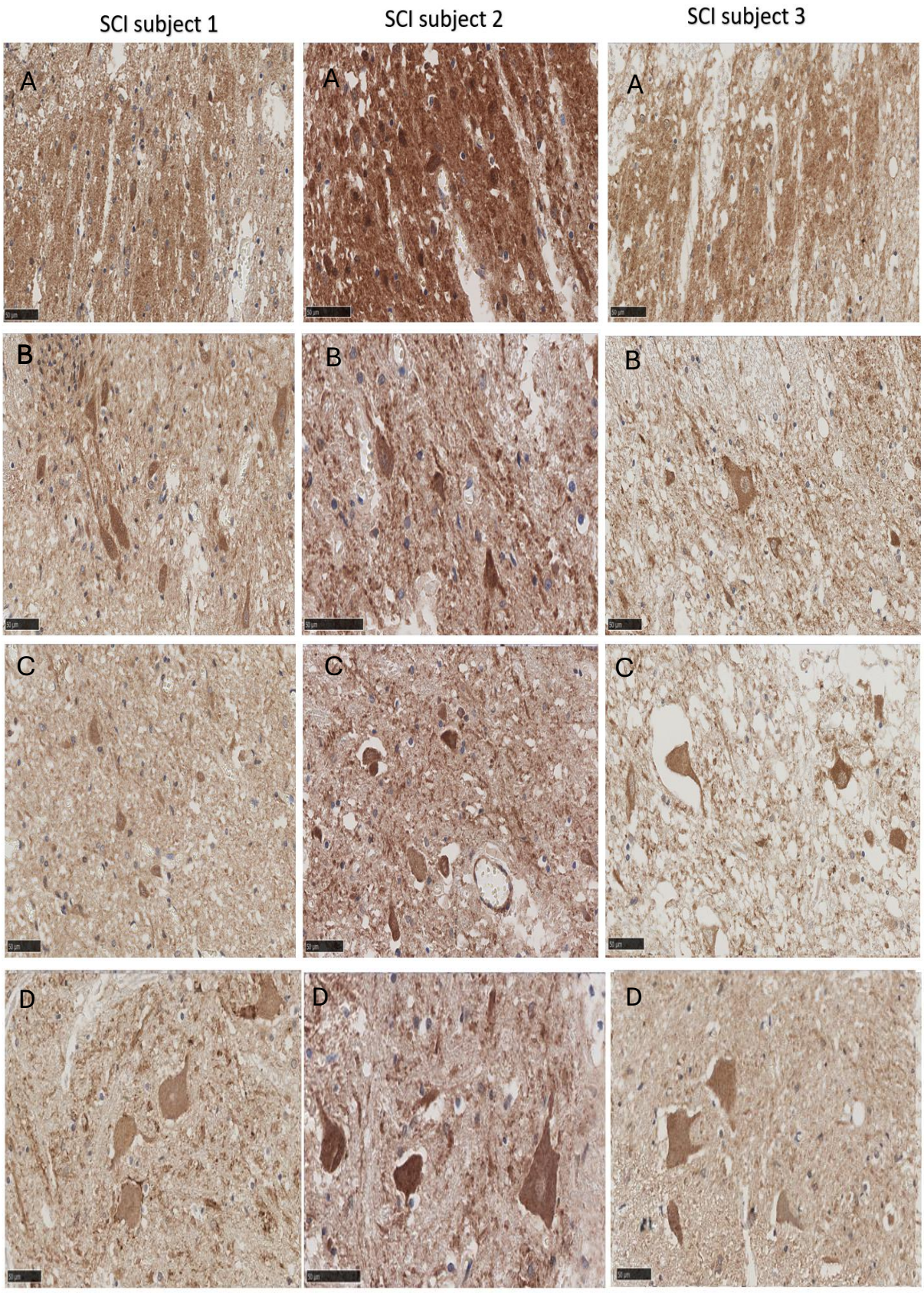
SCI subject 1
SCI subject 2
SCI subject 3
A
A
A
B
B
B
C
C
C
D
D
D

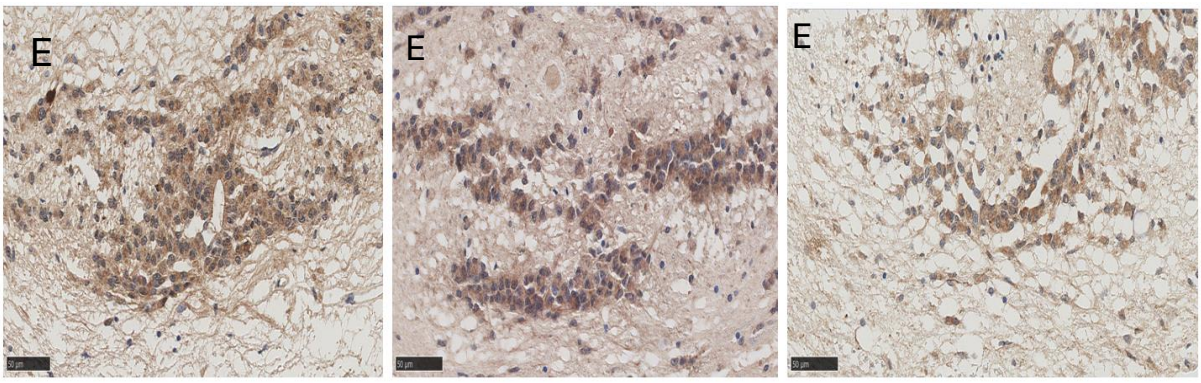

Figure 11. AADC expression in the human spinal cord after SCI*. **A-E** AADC expression pattern in the lumbar spinal gray matter of SCI subjects 1, 2 and 3. **A** AADC immunopositivity in the substantia gelatinosa with membranous and synaptic expression pattern. **B** Base of the dorsal horn and **C** intermediate zone with AADC immunoreactivity in the cytoplasm of neurons as well as on membranes and neuronal processes. **D** Motoneurons with AADC immunoreactivity in the cytoplasm in subject 2 and subject 3, both with chronic SCI. In subject 1 with acute SCI, positive immunoreactivity is mostly detected on membranes and neuronal processes. **E** AADC staining in ependymal cells in the central canal (scale bars 50*μm).

4.2.2. Immunofluorescence

AADC expression on neurons in the human spinal cord was also confirmed by double IF staining of control subject 2. As shown in the figures 12 and 13, AADC co-localized with the neuronal marker SMI32. AADC immunoreactivity was found in the membrane of neurons as well as on neuronal processes.

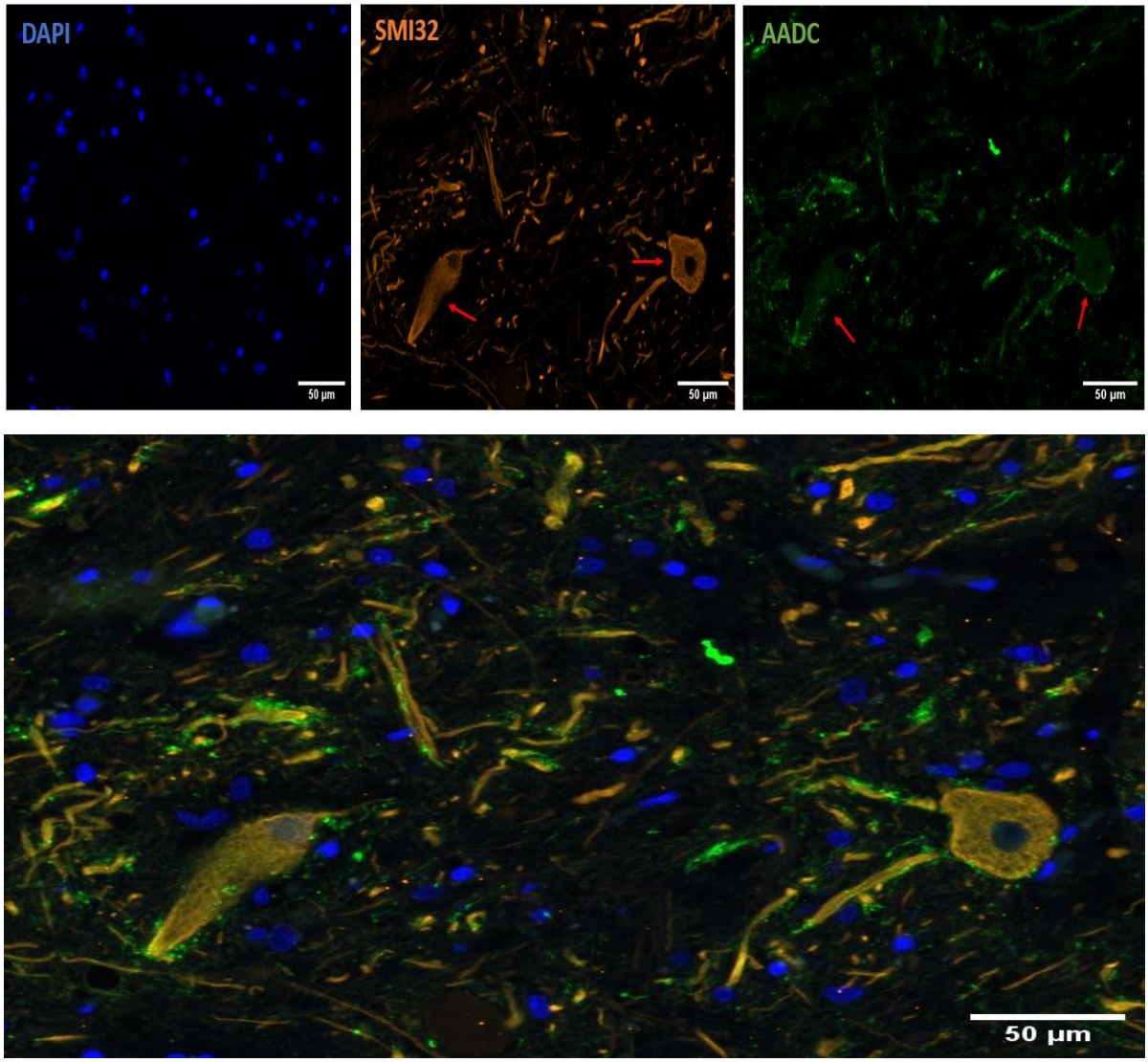

Figure 12. *Co-expression of the neuronal marker SMI32 (orange) and AADC (green) on membranes of motoneurons and on neuronal processes in lamina IX of control subject 2 (scale bars 50 µm).*

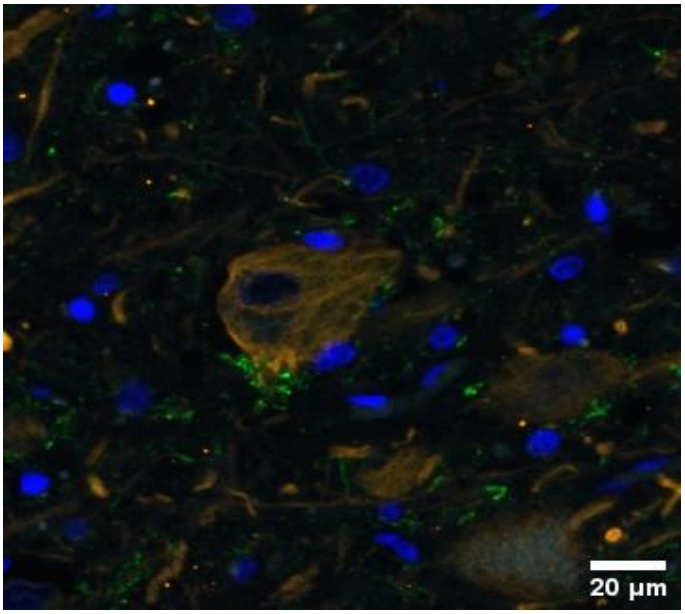

Figure 13. *AADC (green) immunoreactivity on neuronal processes of a SMI32 (orange) labelled neuron, located in the intermediate zone (control subject 2, scale bar 20 µm).*

4.2.3 Statistical analysis of AADC expression and distribution in different spinal cord gray matter regions in control and SCI cases

For the statistical analysis of AADC expression, data from 4 control cases and 3 SCI cases were included. The intensity of the AADC expression was categorized into four levels: no expression, low, medium and strong expression. The total number of cells in various gray matter regions including the dorsal horn, intermediate zone and ventral horn were analyzed. Additionally, specific areas such as the motoneurons of lamina IX in the ventral horn, the substantia gelatinosa corresponding to lamina II in the dorsal horn and lamina X corresponding to the central canal were also examined. The expression levels in the cell body and membrane were analyzed separately. Adjusted residuals with values >2.0 indicate that the expression occurs more frequently than expected under the null hypothesis. Adjusted residuals with values < -2.0 indicate that the expression occurs less frequently than expected under the null hypothesis. Due to the small sample size, only the adjusted residuals were analyzed.

Dorsal horn

A significant association was observed between CNS state (control and SCI) and different AADC expression levels in the membrane in the dorsal horn, X^2 (2) = 113.686, p < .001, Cramer's V = 0.220.

Cells with low expression intensity occurred more frequently than expected under the null hypothesis in the control group (adjusted residual: 7.3) and less frequently in the SCI group (adjusted residual: -7.3). Cells with medium expression intensity were also more frequent in the control group (adjusted residual: 6.1) and less frequent in the SCI group (adjusted residual: -6.1). In contrast, the cells with high expression intensity occurred less frequently than expected in the control group (adjusted residual: -9.1) and more frequently in the SCI group (adjusted residual: 9.1).

There was also a significant association between CNS state (control and SCI) and different AADC expression levels in the cell body, X^2 (2) =113.686, p < .001, Cramer's V = 0.220.

The low expression intensity in the cell body occurred more frequently than expected under the null hypothesis in the controls than in the SCI subjects (adjusted residual: 8.0). Medium expression intensity occurred less frequently than expected in the control group (adjusted residual: -6.7) and more frequently in the SCI group (adjusted residual: 6.7). High expression intensity showed no significant deviation from what is expected under the null hypothesis, with adjusted residuals close to 0 for both, the control (adjusted residual: -1.3) and SCI (adjusted residual: 1.3) groups.

The histograms showing the distribution of AADC expression intensity in the membrane and cell body across CNS states (control and SCI) in the dorsal horn are presented in **Figure 14.**

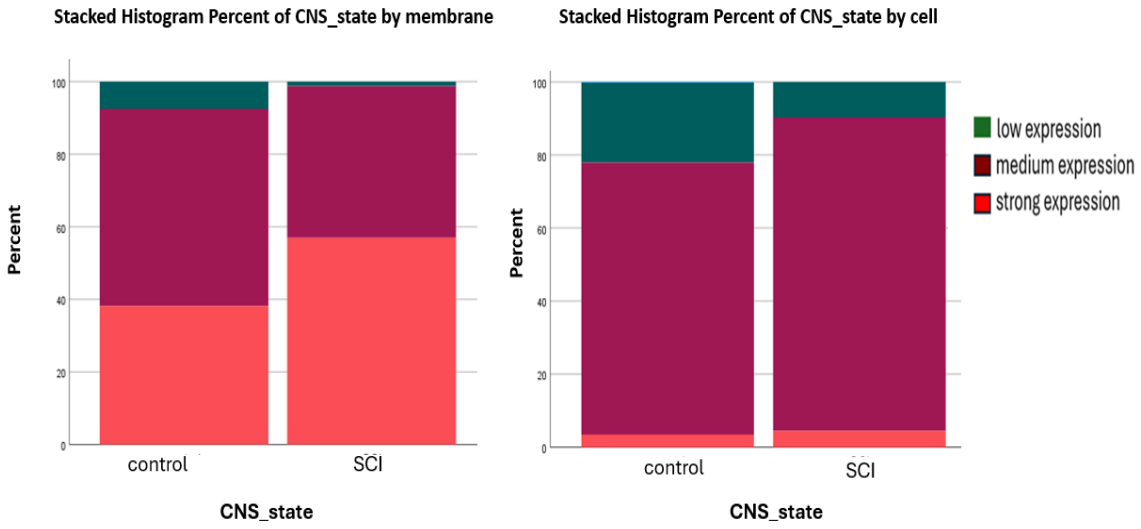

Figure 14. AADC expression intensity in the dorsal horn of control and SCI subjects. *The left panel shows intensity levels of AADC expression within the cell membrane in the dorsal horn for control and SCI cases. The right panel shows intensity levels of AADC expression within the cell body in the dorsal horn for control and SCI cases. The green color indicates low expression, dark red indicates medium expression and red indicates strong expression.*

Intermediate zone

A significant association was observed between CNS state (control and SCI) and different AADC expression levels in the membrane in the intermediate zone, X^2 (2) = 50.267, p < .001, Cramer's V = 0.207.

Cells with low expression intensity occurred more frequently than expected in the control group (adjusted residual: 2.8) and less frequently in the SCI group (adjusted residual: -2.8). Medium expression intensity was also more frequent in the control group (adjusted residual: 5.9) and less frequent in the SCI group (adjusted residual: -5.9). High expression intensity displayed the opposite pattern, occurring less frequently than expected in the control group (adjusted residual: -6.9) and more frequently in the SCI group (adjusted residual: 6.9).

In the cell body, a significant association was found between CNS state (control and SCI) and different AADC expression levels, X^2 (2) = 15.950, p < .001, Cramer's V = 0.116.

Cells with low expression intensity occurred more frequently than expected under the null hypothesis in the control group (adjusted residual: 3.5) and less frequently in the SCI group (adjusted residual: -3.5). Medium expression intensity was observed less frequently than expected in the control group (adjusted residual: -4.0) and more frequently in the SCI group (adjusted residual: 4.0). The high expression intensity did not show a significant deviation from what was expected under the null hypothesis, in the control group (adjusted residual 1.6) and the SCI group (adjusted residual -1.6).

The histograms showing the distribution of AADC expression intensity in the membrane and cell body across CNS states (control and SCI) in the intermediate zone are presented in **Figure 15.**

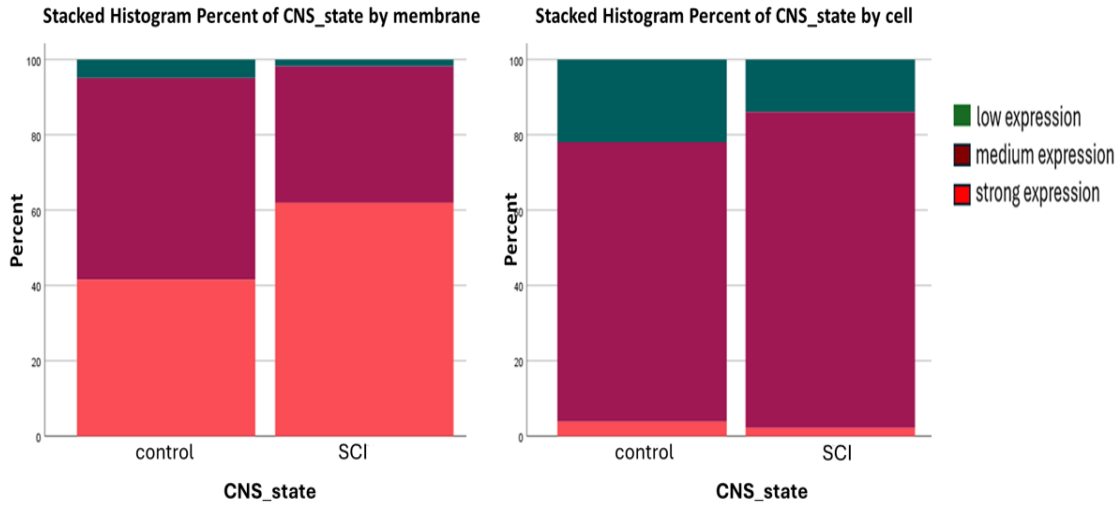

Figure 15. AADC expression intensity in the intermediate zone of control and SCI subjects. *The left panel shows intensity levels of AADC expression within the cell membrane in the intermediate zone for control and SCI cases. The right panel shows intensity levels of AADC expression within the cell body in the intermediate zone for control and SCI cases. The green color indicates low expression, dark red indicates medium expression and red indicates strong expression.*

Ventral horn

A significant association was found between CNS state (control and SCI) and different AADC expression levels in the membrane in the ventral horn, X^2 (2) = 24.333, p < .001, Cramer's V = 0.110.

Cells with low expression intensity occurred more frequently than expected in the control group (adjusted residual: 3.0) and less frequently in the SCI group (adjusted residual: -3.0). Cells with medium expression intensity were observed more frequently in the control group (adjusted residual: 3.5) and less frequently in the SCI group (adjusted residual: -3.5). Cells with high expression intensity showed the opposite pattern, occurring less frequently than expected in the control group (adjusted residual: -4.5) and more frequently in the SCI group (adjusted residual: 4.5).

A significant association was also found between CNS state (control and SCI) and different AADC expression levels in the cell body, X^2 (2) = 62.866, p < .001, Cramer's V = 0.176.

Low expression intensity occurred more frequently than expected in the control group (adjusted residual: 7.8) and less frequently in the SCI group (adjusted residual: -7.8). Medium expression intensity was less frequent than expected in the control group (adjusted residual: -7.6) and more frequent in the SCI group (adjusted residual: 7.6). High expression intensity showed no significant deviation from what was expected under the null hypothesis in the control group (adjusted residual 0.5) and the SCI group (adjusted residual -0.5).

The histograms showing the distribution of AADC expression intensity in the membrane and cell body across CNS states (control and SCI) in the ventral are presented in **Figure 16.**

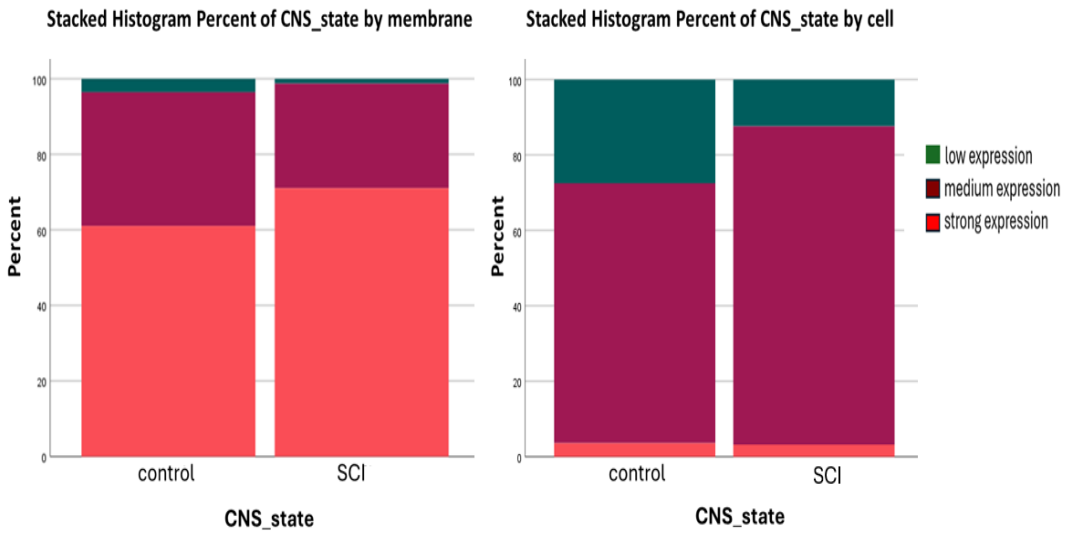

Figure 16. AADC expression intensity in the ventral horn of control and SCI subjects. *The left panel shows intensity levels of AADC expression within the cell membrane in the ventral horn for control and SCI cases. The right panel shows intensity levels of AADC expression within the cell body in the ventral horn for control and SCI cases. The blue color indicates no expression, green indicates low expression, dark red indicates medium expression and red indicates strong expression.*

.

Lamina IX

There was no association between CNS state (control and SCI) and different AADC expression levels in the membrane in lamina IX, $X^2(2) = 4.242$, $p = 0.120$, Cramer's V = 0.146. The Fisher-Freeman-Halton exact test also showed no significant association, with a p-value of 0.123.

Cells with low expression intensity were observed more frequently than expected in the control group (adjusted residual: 1.9) and less frequently in the SCI group (adjusted residual: -1.9). Medium expression intensity occurred less frequently than expected in the control group (adjusted standardized residual: -1.0) and slightly more frequently in the SCI group (adjusted residual: 1.0). High expression intensity showed no significant deviation from what was expected under the null hypothesis in the control group (adjusted residual: 0.3) and the SCI group (adjusted residual: -0.3).

A significant association was found between CNS state (control and SCI) and different AADC expression levels in the cell body, $X^2(1) = 19.837$, $p < .001$, Cramer's V = 0.318.

Low expression intensity occurred more frequently than expected in the control group (adjusted residual: 4.5) and less frequently in the SCI group (adjusted residual: -4.5). Medium expression intensity was observed less frequently than expected in the control group (adjusted residual: -4.5) and more frequently in the SCI group (adjusted residual: 4.5).

The histograms showing the distribution of AADC expression intensity in the membrane and cell body across CNS states (control and SCI) in the lamina IX are presented in **Figure 17.**

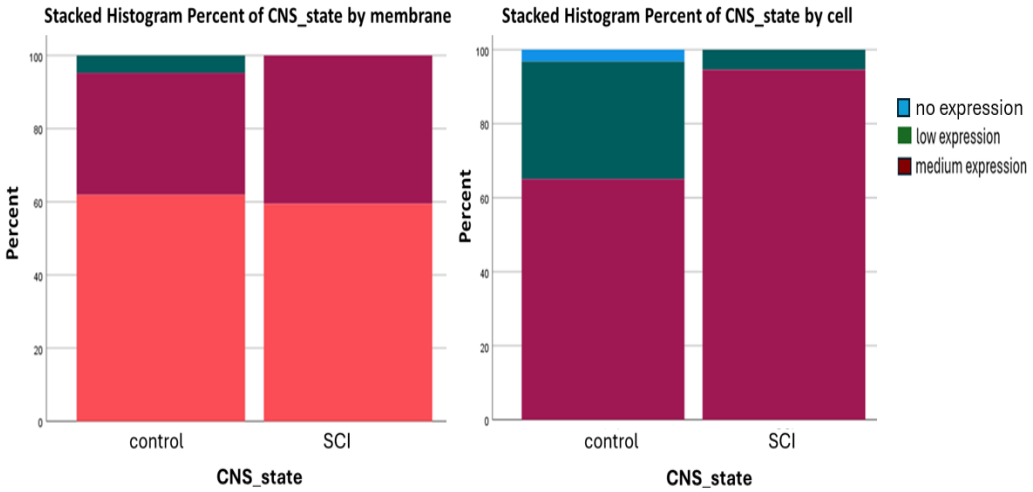

Figure 17. AADC expression intensity in the lamina IX of control and SCI subjects. *The left panel shows intensity levels of AADC expression within the cell membrane in the lamina IX for control and SCI cases. The right panel shows intensity levels of AADC expression within the cell body in the lamina IX for control and SCI cases. The blue color indicates no expression, green indicates low expression, and dark red indicates medium expression.*

In lamina X and substantia gelatinosa, strong expression was observed in both groups across all available samples.

4.3 Expression of DBH in the human spinal cord

4.3.1 Immunohistochemistry

DBH antibody specificity was confirmed by immunohistochemical staining of the locus coeruleus in the brainstem, showing clear neuronal staining **(Figure 14)**.

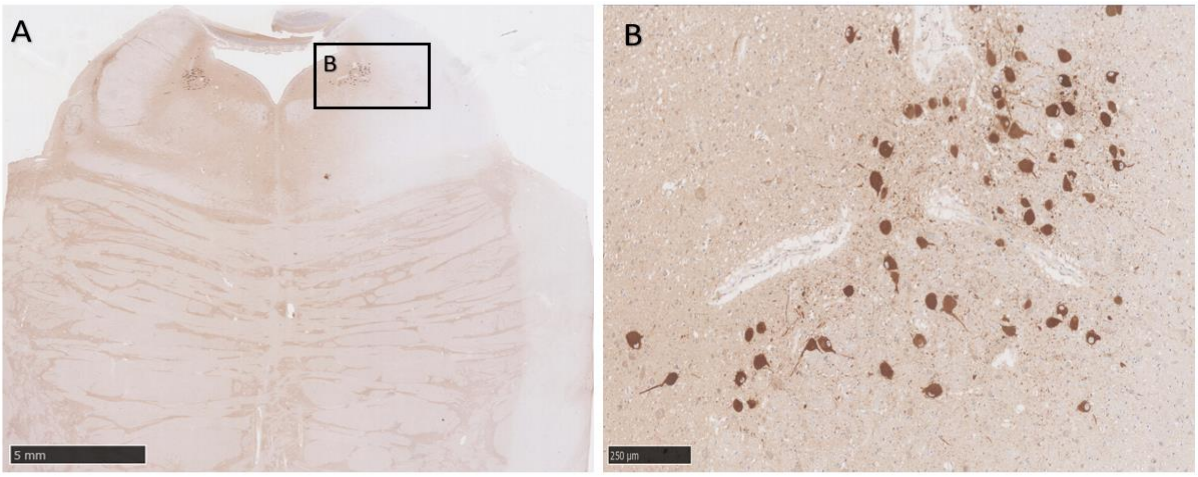

Figure 14. A *DBH immunopositivity in a human brainstem sample.* ***B*** *Locus coeruleus with DBH-immunoreactive neurons.*

In the spinal grey matter, DBH was expressed in the substantia gelatinosa, with the most prominent expression observed in neuronal fibers. In the dorsal horn, DBH expression was evident across all laminae with neurons mostly displaying intermediate cytoplasmic staining and strong cell membrane immunopositivity. The same expression pattern was observed in the intermediate zone and in the ventral horn including motoneurons. Ependymal cells in the central canal displayed DBH immunoreactivity as well **(Figure 15).**

Immunoreactivity was difficult to define due to pronounced unspecific background staining. Despite the use of several pretreatment and blocking protocols, as well as the adjustment of the concentration of the primary antibody, the background staining persisted and could not be effectively reduced.

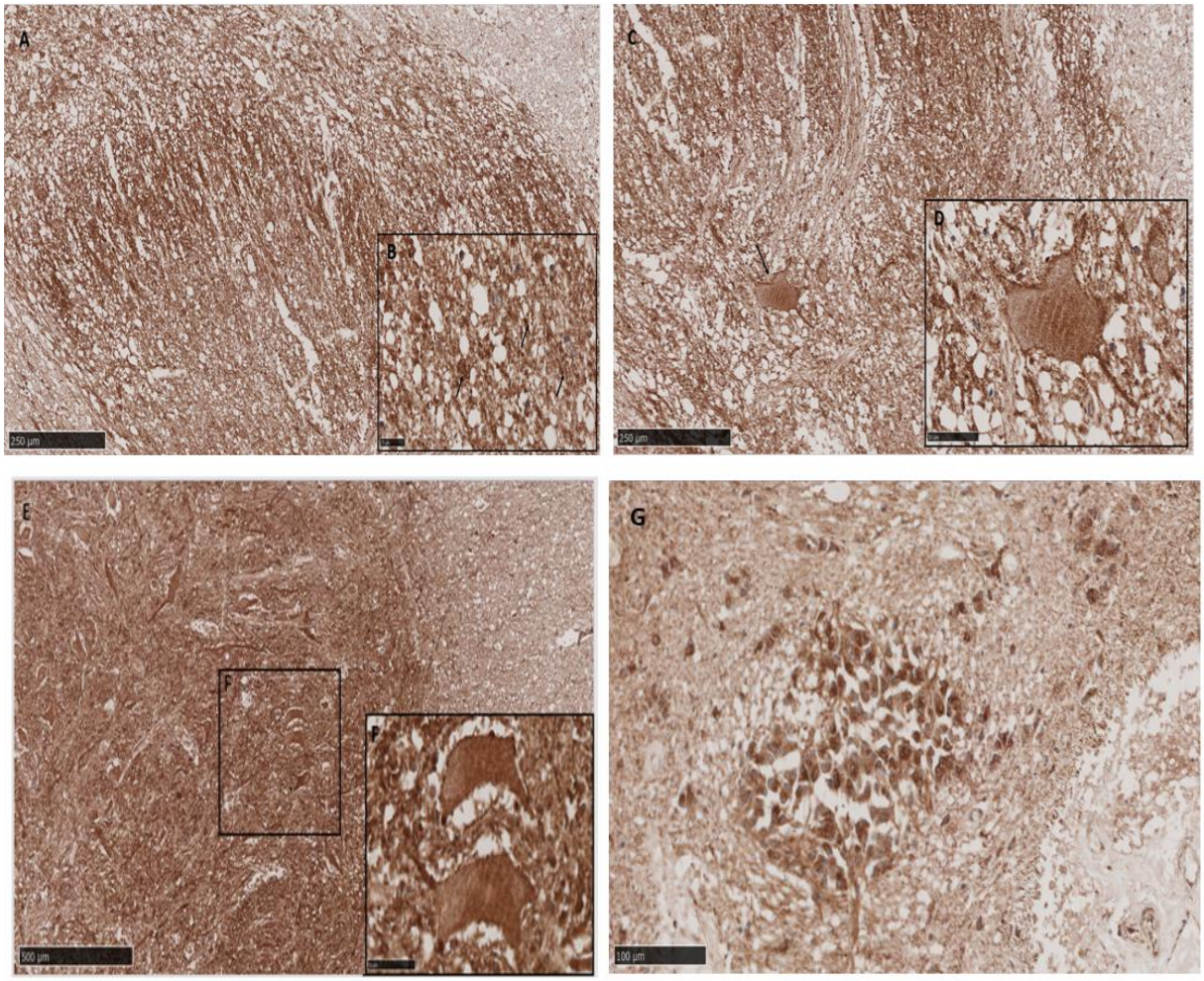

Figure 15.A-B *DBH immunopositivity in the substantia gelatinosa.* ***C-D*** *DBH immunoreactivity in neuronal membranes and neuronal processes in lamina IV in the dorsal horn.* ***E-F*** *DBH immunoreactivity in motoneurons in the ventral horn. The cytoplasm displays a faint staining.* ***G*** *DBH expression in the central canal in lamina X.*

4.3.2. Immunofluorescence

The neuronal marker SMI32 and DBH were co-expressed by immunofluorescence on control spinal cord tissue, confirming DBH immunopositivity on neurons. DBH expression was detected in neuronal membranes and on neuronal processes, although the unspecific background straining interfered with the immunopositivity **(Figures 16 and 17)**.

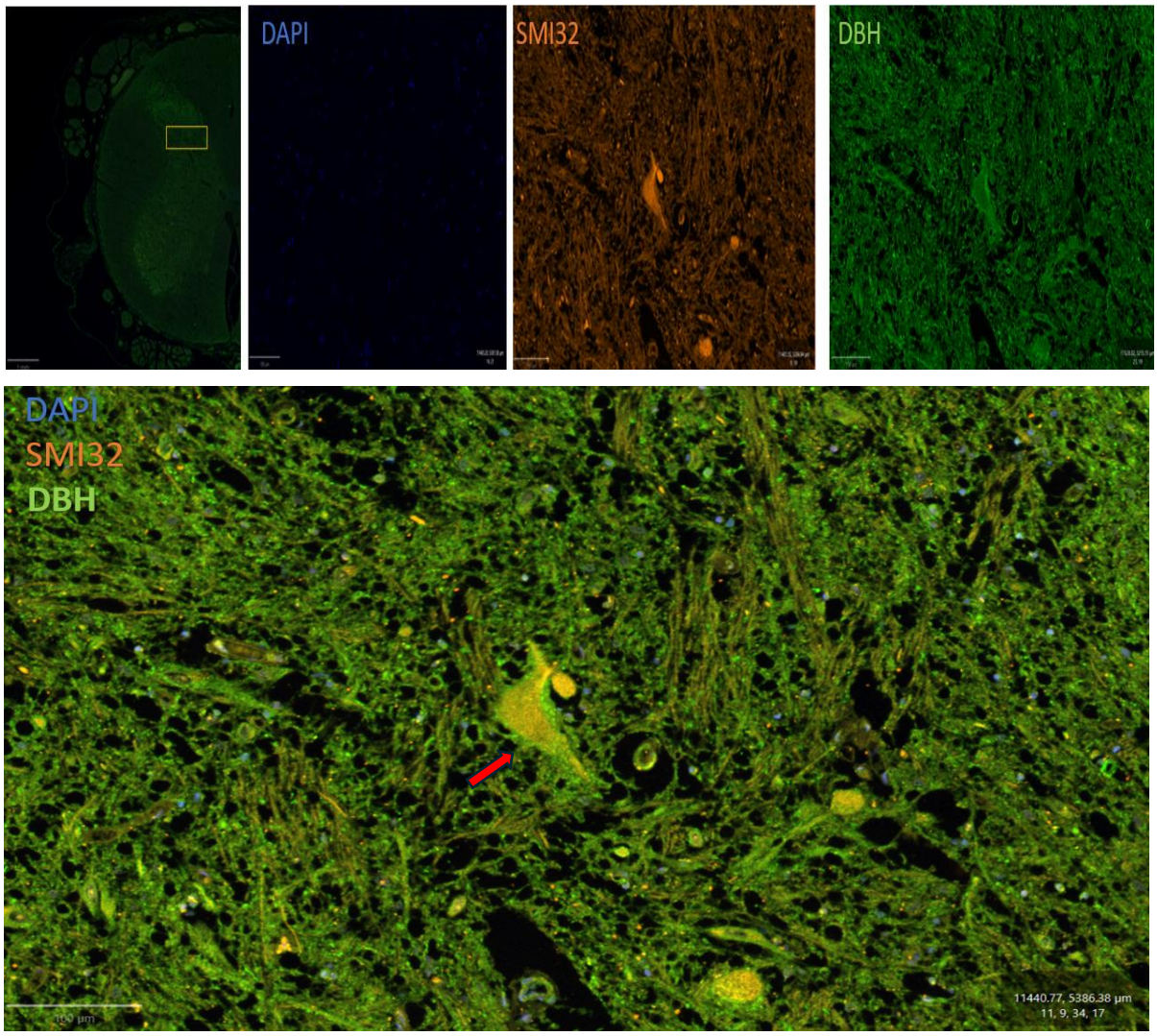

Figure 16. *IF double staining of DBH (green) and SMI32 (orange) in Rexed's lamina IV of control subject 4. The red arrow indicates DBH expression on the neuronal membrane. Nuclear staining with DAPI (blue). Scale bars 100* µm.

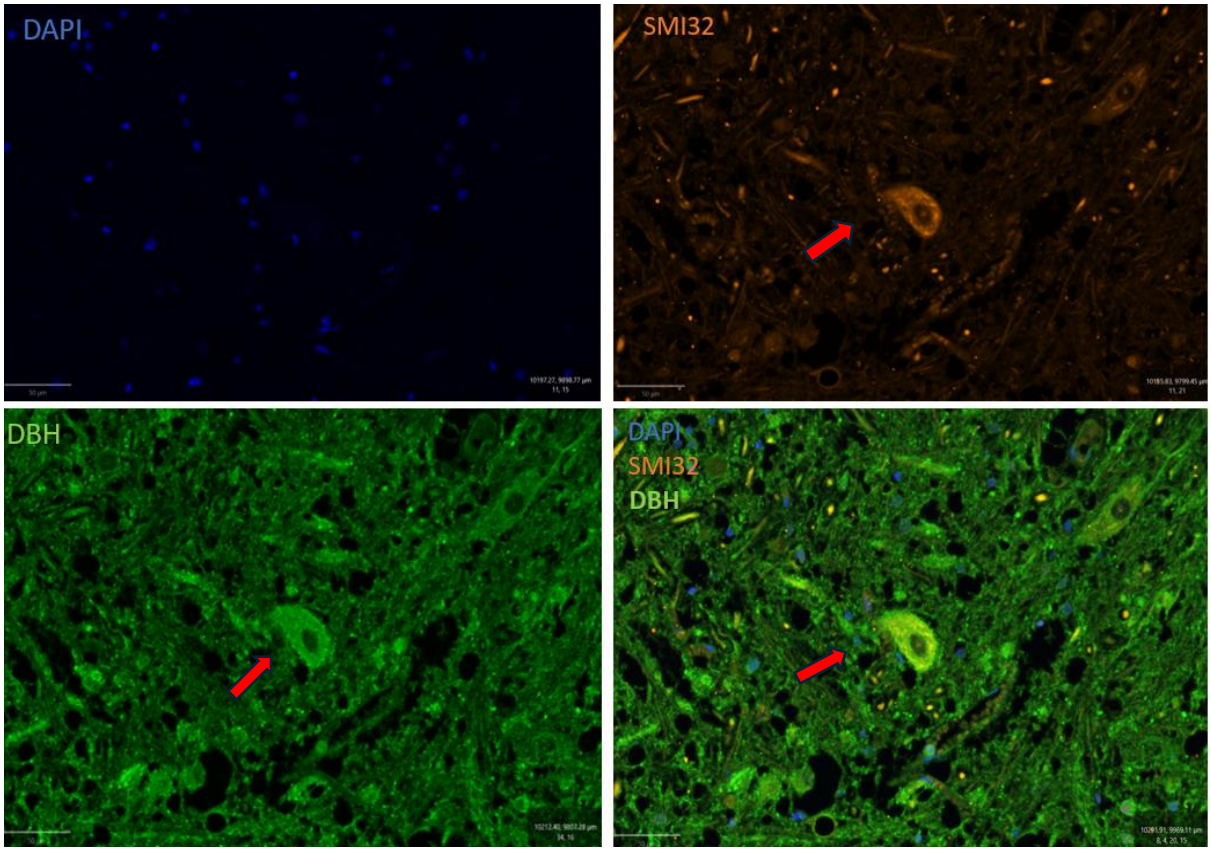

Figure 17.*DBH (green) immunopositivity on the membrane of a motoneuron, indicated by red arrows. SMI32 expression (orange) confirmed the neuronal identity of the cell. Nuclei were stained with DAPI (blue). Scale bars 50 µm.*

4.4 Western blot

Western blot analysis was performed to detect the expression of D1 and D2 receptors as well as DAT in intact human lumbar spinal cord tissue.

4.4.1 D1 receptor

To optimize Western blotting conditions, considerable effort was devoted to identifying the most effective blocking solution for each target protein. To minimize non-specific binding and background staining we systematically evaluated various blocking agents, including milk, bovine serum, and Every

Blot Blocking Buffer (BIO-RAD). The optimal blocking solution for the D1 receptor was Every Blot Blocking Buffer.

The specific band of the D1 receptor was detected in intact human lumbar spinal cord tissue in the western blot, within three different concentrations of protein extract loaded on the gel. Human substantia nigra was used as a positive control. Clear bands of the D1 receptor were observed around 55 kDa, consistent with the molecular weight predictions provided by UniProt **(Figure 18).**

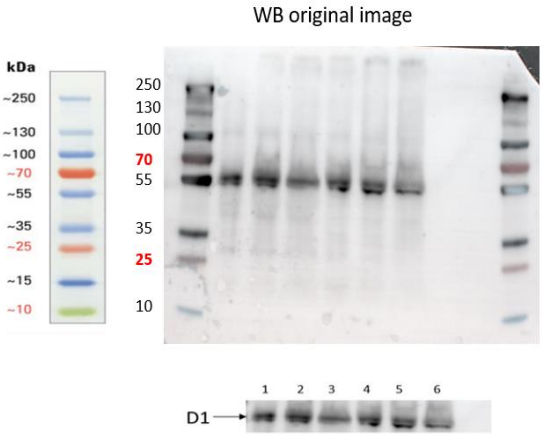

Figure 18. 1, 2 and 3 - *Human spinal cord with protein extract volumes of 30, 40 and 60 µg, respectively.* ***4, 5 and 6*** *- substantia nigra positive control with protein extract volumes of 30, 40 and 60 µg, respectively.*

4.4.2 D2 receptor

Several bands of the D2 receptor were detected in human spinal cord tissue, including a band consistent with the molecular weight of 50 kDa, as predicted by UniProt. However, the western blot also showed the presence of additional bands, probably due to non-specific binding of the primary antibody, making interpretation of the results difficult. Increasing the concentration of the primary antibody as well as the duration of the blocking and washing steps did not improve results. Human hippocampus was used as a positive control **(Figure 19).**

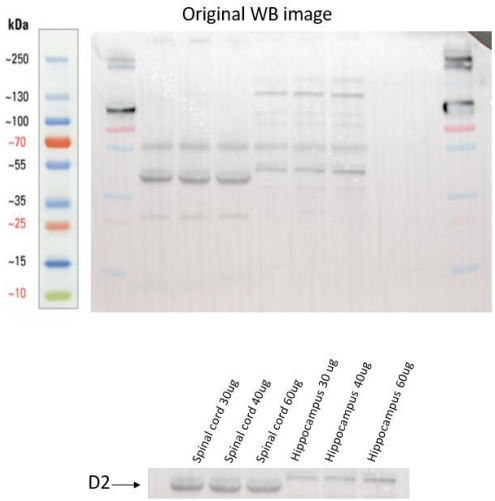

Figure 19. *Western blot detection of the D2 receptor in the human spinal cord.* ***1, 2 and 3*** *Human spinal cord with protein extract volumes of 30, 40 and 60 µg respectively).* ***4, 5 and 6*** *Hippocampus positive control with protein extract volumes of 30, 40 and 60 µg respectively.*

4.4.3 DAT

The resulting blot showed the presence of several faint bands for DAT in the intact human spinal cord. Human substantia nigra was used as a positive control. According to UniProt, the predicted molecular weight of DAT is approximately 88 kDa. The molecular weight of the strongest bands detected in the substantia nigra, approximately 50 kDa differed from the molecular weight of the strongest bands detected in the spinal cord, approximately 70 kDa **(Figure 20).**

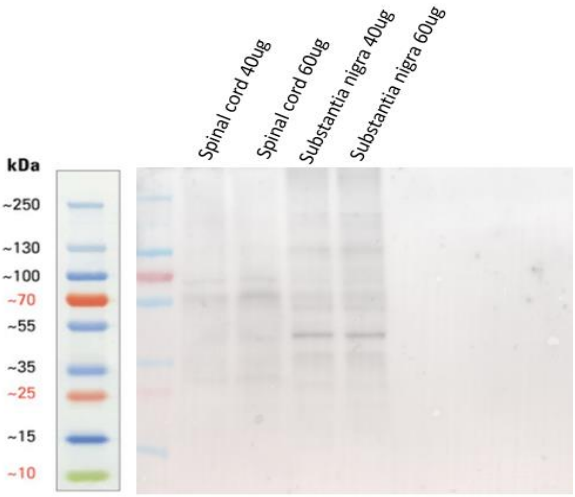

Figure 20.*Western blot detection of DAT in the human spinal cord.Human spinal cord with protein extract volumes of 40 and 60 µg respectively as well as substantia nigra positive control with protein extract volumes of 40 and 60 µg respectively.*

5. Discussion

The objective of this study was to investigate the presence and localization of key catecholaminergic enzymes TH, DBH, and AADC as well as the dopaminergic receptors D1, D2, and the dopaminergic transporter DAT in the intact human lumbar spinal cord. TH and AADC were also investigated in the human lumbar spinal cord after sustained SCI and the injury-related alterations were compared to intact human spinal cord samples.

5.1 TH expression in the human spinal cord

This is the first study to demonstrate the presence of TH in the human lumbar spinal cord, both in intact and injured spinal cord tissue. TH was expressed in the axonal terminals of the intact spinal cord throughout the gray matter. This suggests that TH expression is largely restricted to the presynaptic terminals of axons originating from supraspinal sources. This finding is consistent with the results of Barraud et al.[51] who showed that dopaminergic A11 neurons are the only TH-expressing cell group projecting to the spinal cord in non-human primates who showed that dopaminergic A11 neurons are the only TH-expressing cell group projecting to the spinal cord in non-human primates. The absence

of TH expression on axonal terminals in cases with chronic SCI as well as the absence of TH in spinal neurons in the intact and injured spinal cord supports the hypothesis that spinal TH depends on supraspinal inputs.

In the subject with acute SCI, TH was only weakly expressed on axonal terminals in the dorsal horn and intermediate zone. This suggests that in the early stages of SCI, some descending axonal fibers are transiently preserved and continue to have some influence on catecholaminergic neurotransmission in the spinal cord until they degenerate over time. Furthermore, the results are in partial agreement with those of Hou et al.[64] who showed that TH is expressed in axonal fibres as well as in neuronal somata in the intact spinal cord of rats. Interestingly, they reported an increase of TH-positive neurons in the lumbosacral region after thoracic transection. In agreement with the current study, they also showed that axonal TH-positive fibres disappeared with injury. The absence of TH-positive neuronal cells in the current study can be explained by interspecies differences regarding the anatomical and functional organization of the human and rat spinal cord.

5.2 AADC expression in the human spinal cord

This study represents the first systematic analysis of AADC expression on protein level in the human lumbar spinal cord. To understand the potential role of AADC in dopamine synthesis following SCI, the AADC expression was investigated in the spinal cord of subjects with intact spinal cord as well as after sustained SCI.

In both control and SCI subjects, AADC was expressed in the dorsal horn, the intermediate zone, and the ventral horn. These results indicate a more extensive distribution of AADC immunopositivity than previously reported in rats[44]. The findings of the current study thus align with multiple studies that have demonstrated the presence of AADC neurons not only in the vicinity of the central canal in lamina X of the rat spinal cord, but also in the dorsal horn, intermediate zone and ventral horn[42,43,65,66].

In control subjects, AADC was localized predominantly in neuronal membranes and processes throughout the spinal gray matter. The subject with acute SCI showed a similar expression pattern to the control group indicating that immediate changes post-injury did not significantly alter AADC expression. However, in subjects with chronic SCI, there was an increase in AADC immunopositivity within the cytoplasm of neurons and a marked decrease in membrane expression in the dorsal horn, the intermediate zone and the ventral horn.

The observed shift in AADC expression after SCI may be considered as an adaptive response to the injury. This finding has an important therapeutic value due to the fact that the conversion of L-DOPA to dopamine by AADC is possible at the spinal level below the lesion, supporting spinal neurons to maintain their functionality and plasticity despite the disruption of dopaminergic pathways. This is consistent with studies in rat models showing that AADC retains its enzymatic activity and can synthesize monoamines at the spinal level below the lesion after exogenous application of the monoamine precursors[65,66]. However, the qualitative analysis in the present study does not align with the quantitative assessment of the expression levels in the cell body and the cell membrane for both groups. These discrepancies may be attributed to the small sample size and inter-subject variability within the SCI group.

5.3 DBH expression in the human spinal cord

Furthermore, the current study provided insights into the expression and localization of DBH in the intact human spinal cord. DBH immunopositivity was found on neuronal processes throughout the entire spinal gray matter, including the dorsal horn, intermediate zone and the ventral horn of the spinal cord. These findings are consistent with those observed in animal studies, providing further evidence that supports the hypothesis that DBH in the intact spinal cord depends on supraspinal inputs. Westlund et al.[28,30] observed DBH expression in neuronal fibres of the dorsal horn, intermediate zone and ventral horn, as well as around the central canal of the spinal cord in rats and non-human primates. These observations were further confirmed and extended by Cassam et al.[48,67] who demonstrated that DBH immunoreactivity was predominantly localized to neuronal fibers throughout the entire gray matter in the intact rat spinal cord, as previously described. Moreover, a loss or significant decrease in immunoreactive DBH fibres caudal to the transection was also observed, followed by an increase in DBH-expressing neuronal somata in chronic spinal rats. This finding indicates that spinal neurons in rats respond to injury by increasing local DBH production caudal to the site of transection.

Further research is necessary to determine whether the adaptive mechanisms to SCI, as observed in rats, are also present in the human spinal cord. This knowledge is essential for developing therapeutic strategies that will enable the maintenance of noradrenergic modulation in the spinal cord, despite the disruption of noradrenergic pathways, and contribute to neuroplasticity and recovery after injury.

5.4 D1 receptor, D2 receptor and DAT in human spinal cord

To gain a more comprehensive understanding of the functioning of the dopaminergic system within the intact human spinal cord, the expression of DAT, D1 and D2 receptors was examined. Synthesized dopamine binds to D1 and D2 receptors to exert its activity in postsynaptic neurons, and is then recycled by the presynaptic neuron through reuptake by DAT[68,69]. D2 receptors are also found presynaptically where they increase the rate of dopamine uptake by increasing the activity of existing DAT and expression of DAT on the plasma membrane[69]. The activation of D2 receptors on presynaptic terminals inhibits TH activity that regulates dopamine synthesis[69]. Therefore, examining the expression of these proteins is crucial for understanding the function of dopaminergic neurotransmission in the spinal cord, particularly in the context of injury-related processes and motor control.

D1 and D2 receptors have been demonstrated in the spinal cord of rats[55] and mice[53]. The presence of the D2 receptor was also confirmed in the lumbar spinal cord of non-human primates while the D1 receptor was not expressed[51]. The current study is the first to examine the expression of these receptors at the protein level in the intact human spinal cord. The detection of the targets was achieved through the Western blot technique. The antibody used for the D2 receptors targets both presynaptically and postsynaptically expressed D2 receptors.

According to the Uniprot database, the D1 and D2 receptors have a calculated molecular weight of 55 and 50 kDa, respectively. The results of the current study align with those previously reported by Li Z, et al.[70] who observed the expression of D1 and D2 receptors in the brain of rats, with a molecular weight of approximately 55 kDa for D1 and 50 kDa for D2. In the current study, D2 was presented with two bands. This is consistent with the findings of Lindgren et al.[71] and Mei C et al.[72] who reported that D2 receptors have two isoforms, the short (D2S) and the long (D2L), which are generated by differential splicing of the same gene. The different isoforms of the D2 receptor play different roles in dopaminergic signaling[71,72]. Therefore, it would be interesting for future studies to look at the topographical expression of these receptor isoforms in the human spinal cord.

The Western blot analysis of the current study of DAT expression in intact human spinal cord and substantia nigra showed the presence of multiple faint bands whose molecular weight was not consistent with the predicted Uniprot molecular weight (88kDa). The detection of DAT in the spinal cord across other studies demonstrated variability. Koblinger K, et al.[52] showed that dopaminergic pathways projecting to the spinal cord of mice lack DAT expression. The absence of DAT was also confirmed in the spinal cord of non-human primates[73]. Conversely, Kim et al. [73]

demonstrated spinal DAT immunoreactivity in the dorsal horn of mice and reported its role in plasticity. A possible explanation for the inconclusive DAT expression in the current study may be the low expression level of DAT in the spinal cord, which cannot be detected by Western blot due to low sensitivity of the method or the application of an inappropriate antibody for Western blotting since there were also discrepancies regarding the molecular weight of the bands found in the positive control. An additional potential explanation for the low expression for spinal DAT may be the existence of an alternative reuptake mechanism, as evidenced in mice. A study conducted by Morón JA et al.[74]. demonstrated that dopamine uptake in the brain of mice can be facilitated by the noradrenaline transporter (NET) in the absence of DAT.

Nevertheless, the inconclusive results regarding the detection of DAT in the positive control samples of the current study indicate the need for further optimization of the detection method or the use of other detection methods, such as immunohistochemistry or even detection at the mRNA level by qPCR or sequencing methods to validate the results.

5.5 Limitations

The small sample size for the statistical analysis of AADC expression is one of the major limitations of the current study. The results for DBH should be interpreted with caution because they were obtained from only one intact spinal cord sample.

The presence of multiple bands of D2 raises questions about the specificity of the antibody used in the study. The absence of DAT in the substantia nigra, which has been reported to be a region of high DAT expression, also indicates the need for antibody validation and optimisation of Western blotting conditions. To fully understand the dopaminergic system within the human spinal cord, it is also necessary to further investigate how SCI affects the expression of D1 and D2 receptors and DAT.

Conclusion

This study represents the initial investigation of the catecholamine system in the human spinal cord. The results presented provide important insights into dopaminergic and noradrenergic signaling in the human spinal cord. The detection of the catecholaminergic enzymatic machinery, including TH, AADC and DBH in the intact human lumbar spinal cord, suggests that they are involved in spinal sensorimotor

control. The shift in AADC expression observed after sustained SCI suggests an adaptive response in the spinal gray matter to injury, possibly through the increased local production of dopamine. The existence of AADC cells below a spinal cord lesion is promising for the therapeutic use of precursor drugs such as L-DOPA, which can cross the blood-brain barrier, penetrate the spinal cord, and stimulate the local production of dopamine.

References

1. Minassian, K., Hofstoetter, U. S., Dzeladini, F., Guertin, P. A. & Ijspeert, A. The Human Central Pattern Generator for Locomotion: Does It Exist and Contribute to Walking? *The Neuroscientist* **23**, 649–663 (2017).

2. Sharples, S. A., Koblinger, K., Humphreys, J. M. & Whelan, P. J. Dopamine: a parallel pathway for the modulation of spinal locomotor networks. *Front Neural Circuits* **8**, (2014).

3. Jordan, L. M., Liu, J., Hedlund, P. B., Akay, T. & Pearson, K. G. Descending command systems for the initiation of locomotion in mammals. *Brain Res Rev* **57**, 183–191 (2008).

4. Fernstrom, J. D. & Fernstrom, M. H. Tyrosine, Phenylalanine, and Catecholamine Synthesis and Function in the Brain2. *J Nutr* **137**, 1539S-1547S (2007).

5. Peaston, R. T. & Weinkove, C. Measurement of catecholamines and their metabolites. *Annals of Clinical Biochemistry: International Journal of Laboratory Medicine* **41**, 17–38 (2004).

6. Bingham, W. G., Ruffolo, R. & Friedman, S. J. Catecholamine levels in the injured spinal cord of monkeys. *J Neurosurg* **42**, 174–178 (1975).

7. McGeer, E. G. & McGeer, P. L. CATECHOLAMINE CONTENT OF SPINAL CORD. *Can J Biochem Physiol* **40**, 1141–1151 (1962).

8. Kobayashi, K. Role of Catecholamine Signaling in Brain and Nervous System Functions: New Insights from Mouse Molecular Genetic Study. *Journal of Investigative Dermatology Symposium Proceedings* **6**, 115–121 (2001).

9. Andén, N., Häggendal, J., Magnusson, T. & Rosengren, E. The Time Course of the Disappearance of Noradrenaline and 5-Hydroxytryptamine in the Spinal Cord after Transection. *Acta Physiol Scand* **62**, 115–118 (1964).

10. Hains, B. C., Black, J. A. & Waxman, S. G. Primary cortical motor neurons undergo apoptosis after axotomizing spinal cord injury. *Journal of Comparative Neurology* **462**, 328–341 (2003).

11. Grahn, P. J. *et al.* Restoration of motor function following spinal cord injury via optimal control of intraspinal microstimulation: toward a next generation closed-loop neural prosthesis. *Front Neurosci* **8**, (2014).

12. Commissiong, J. W. The synthesis and metabolism of catecholamines in the spinal cord of the rat after acute and chronic transections. *Brain Res* **347**, 104–111 (1985).

13. Commissiong, J. W. & Sedgwick, E. M. DOPAMINE AND NORADRENALINE IN HUMAN SPINAL CORD. *The Lancet* **305**, 347 (1975).

14. Scatton, B. *et al.* Degeneration of noradrenergic and serotonergic but not dopaminergic neurones in the lumbar spinal cord of parkinsonian patients. *Brain Res* **380**, 181–185 (1986).

15. Lawhead, R. G., Blaxall, H. S. & Bylund, D. B. α-2A Is the Predominant α-2 Adrenergic Receptor Subtype in Human Spinal Cord. *Anesthesiology* **77**, 983–991 (1992).

16. Smith, M. S. *et al.* α2-Adrenergic receptors in human spinal cord: specific localized expression of mRNA encoding α2-adrenergic receptor subtypes at four distinct levels. *Molecular Brain Research* **34**, 109–117 (1995).

17. Smith, M. S., Schambra, U. B., Wilson, K. H., Page, S. O. & Schwinn, D. A. α1-Adrenergic receptors in human spinal cord: specific localized expression of mRNA encoding α1-adrenergic receptor subtypes at four distinct levels. *Molecular Brain Research* **63**, 254–261 (1999).

18. Anatomy and Physiology of the Spinal Cord. in *Essentials of Spinal Cord Injury* (eds. Fehlings, M. G. et al.) (Georg Thieme Verlag, Stuttgart, 2013). doi:10.1055/b-0034-83843.

19. Hochman, S. Spinal cord. *Current Biology* **17**, R950–R955 (2007).

20. Bican, O., Minagar, A. & Pruitt, A. A. The Spinal Cord. *Neurol Clin* **31**, 1–18 (2013).

21. Cho, T. A. Spinal Cord Functional Anatomy. *CONTINUUM: Lifelong Learning in Neurology* **21**, 13–35 (2015).

22. Khalid, S. & Tubbs, R. S. Neuroanatomy and Neuropsychology of Pain. *Cureus* (2017) doi:10.7759/cureus.1754.

23. NAGATSU, T. The catecholamine system in health and disease -Relation to tyrosine 3-monooxygenase and other catecholamine-synthesizing enzymes-. *Proceedings of the Japan Academy, Series B* **82**, 388–415 (2006).

24. Goldstein, D. S. Noradrenergic Neurotransmission. in *Primer on the Autonomic Nervous System* 37–43 (Elsevier, 2012). doi:10.1016/B978-0-12-386525-0.00006-8.

25. Peaston, R. T. & Weinkove, C. Measurement of catecholamines and their metabolites. *Annals of Clinical Biochemistry: International Journal of Laboratory Medicine* **41**, 17–38 (2004).

26. Grealish, S. *et al.* The A9 dopamine neuron component in grafts of ventral mesencephalon is an important determinant for recovery of motor function in a rat model of Parkinson's disease. *Brain* **133**, 482–495 (2010).

27. Björklund, A. & Skagerberg, G. Evidence for a major spinal cord projection from the diencephalic A11 dopamine cell group in the rat using transmitter-specific fluorescent retrograde tracing. *Brain Res* **177**, 170–175 (1979).

28. Westlund, K. N., Bowker, R. M., Ziegler, M. G. & Coulter, J. D. Origins and terminations of descending noradrenergic projections to the spinal cord of monkey. *Brain Res* **292**, 1–16 (1984).

29. Westlund, K. N., Bowker, R. M., Ziegler, M. G. & Coulter, J. D. Origins of spinal noradrenergic pathways demonstrated by retrograde transport of antibody to dopamine-β-hydroxylase. *Neurosci Lett* **25**, 243–249 (1981).

30. Westlund, K. N., Bowker, R. M., Ziegler, M. G. & Coulter, J. D. Noradrenergic projections to the spinal cord of the rat. *Brain Res* **263**, 15–31 (1983).

31. Holland, N., Robbins, T. W. & Rowe, J. B. The role of noradrenaline in cognition and cognitive disorders. *Brain* **144**, 2243–2256 (2021).

32. Babić Leko, M., Hof, P. R. & Šimić, G. Alterations and interactions of subcortical modulatory systems in Alzheimer's disease. in 379–421 (2021). doi:10.1016/bs.pbr.2020.07.016.

33. Kiehn, O., Sillar, K. T., Kjaerulff, O. & McDearmid, J. R. Effects of Noradrenaline on Locomotor Rhythm–Generating Networks in the Isolated Neonatal Rat Spinal Cord. *J Neurophysiol* **82**, 741–746 (1999).

34. Jordan, L. M., Liu, J., Hedlund, P. B., Akay, T. & Pearson, K. G. Descending command systems for the initiation of locomotion in mammals. *Brain Res Rev* **57**, 183–191 (2008).

35. Barbeau, H. & Rossignol, S. Initiation and modulation of the locomotor pattern in the adult chronic spinal cat by noradrenergic, serotonergic and dopaminergic drugs. *Brain Res* **546**, 250–260 (1991).

36. Holstege, J. C. *et al.* Distribution of dopamine immunoreactivity in the rat, cat, and monkey spinal cord. *J Comp Neurol* **376**, 631–652 (1996).

37. Yokota, K. *et al.* Pathological changes of distal motor neurons after complete spinal cord injury. *Mol Brain* **12**, 4 (2019).

38. David, S., López-Vales, R. & Wee Yong, V. Harmful and beneficial effects of inflammation after spinal cord injury. in 485–502 (2012). doi:10.1016/B978-0-444-52137-8.00030-9.

39. Hou, S. *et al.* Dopamine is produced in the rat spinal cord and regulates micturition reflex after spinal cord injury. *Exp Neurol* **285**, 136–146 (2016).

40. Liu, Y. *et al.* Metabolism and secretion mechanism of catecholamine syndrome and related treatment strategies. *J Xiangya Med* **5**, 39–39 (2020).

41. Morón, J. A., Brockington, A., Wise, R. A., Rocha, B. A. & Hope, B. T. Dopamine Uptake through the Norepinephrine Transporter in Brain Regions with Low Levels of the Dopamine Transporter: Evidence from Knock-Out Mouse Lines. *The Journal of Neuroscience* **22**, 389–395 (2002).

42. Ren, L.-Q. *et al.* Heterogenic Distribution of Aromatic L-Amino Acid Decarboxylase Neurons in the Rat Spinal Cord. *Front Integr Neurosci* **11**, (2017).

43. Ren, L.-Q., Wienecke, J., Hultborn, H. & Zhang, M. Production of Dopamine by Aromatic <scp>l</scp> -Amino Acid Decarboxylase Cells after Spinal Cord Injury. *J Neurotrauma* **33**, 1150–1160 (2016).

44. Jaeger, C. B. *et al.* Some Neurons of the Rat Central Nervous System Contain Aromatic-L-Amino-Acid Decarboxylase But Not Monoamines. *Science (1979)* **219**, 1233–1235 (1983).

45. Weihe, E., Depboylu, C., Schütz, B., Schäfer, M. K.-H. & Eiden, L. E. Three Types of Tyrosine Hydroxylase-Positive CNS Neurons Distinguished by Dopa Decarboxylase and VMAT2 Co-Expression. *Cell Mol Neurobiol* **26**, 657–676 (2006).

46. Westlund, K. N., Bowker, R. M., Ziegler, M. G. & Coulter, J. D. Origins and terminations of descending noradrenergic projections to the spinal cord of monkey. *Brain Res* **292**, 1–16 (1984).

47. Westlund, K. N., Bowker, R. M., Ziegler, M. G. & Coulter, J. D. Noradrenergic projections to the spinal cord of the rat. *Brain Res* **263**, 15–31 (1983).

48. Cassam, A. K., Rogers, K. A. & Weaver, L. C. Co-localization of substance P and dopamine β-hydroxylase with growth-associated protein-43 is lost caudal to a spinal cord transection. *Neuroscience* **88**, 1275–1288 (1999).

49. Bu, M., Farrer, M. J. & Khoshbouei, H. Dynamic control of the dopamine transporter in neurotransmission and homeostasis. *NPJ Parkinsons Dis* **7**, 22 (2021).

50. Vaughan, R. A. & Foster, J. D. Mechanisms of dopamine transporter regulation in normal and disease states. *Trends Pharmacol Sci* **34**, 489–496 (2013).

51. Barraud, Q. *et al.* Neuroanatomical Study of the A11 Diencephalospinal Pathway in the Non-Human Primate. *PLoS One* **5**, e13306 (2010).

52. Koblinger, K. *et al.* Characterization of A11 Neurons Projecting to the Spinal Cord of Mice. *PLoS One* **9**, e109636 (2014).

53. Zhu, H., Clemens, S., Sawchuk, M. & Hochman, S. Expression and distribution of all dopamine receptor subtypes (D1–D5) in the mouse lumbar spinal cord: A real-time polymerase chain reaction and non-autoradiographic in situ hybridization study. *Neuroscience* **149**, 885–897 (2007).

54. Pappas, S. S., Behrouz, B., Janis, K. L., Goudreau, J. L. & Lookingland, K. J. Lack of D2 receptor mediated regulation of dopamine synthesis in A11 diencephalospinal neurons in male and female mice. *Brain Res* **1214**, 1–10 (2008).

55. Dubois, A., Savasta, M., Curet, O. & Scatton, B. Autoradiographic distribution of the D1 agonist [3H]SKF 38393, in the rat brain and spinal cord. Comparison with the distribution of D2 dopamine receptors. *Neuroscience* **19**, 125–137 (1986).

56. Xu, Y. *et al.* Tyrosine mRNA is expressed in human substantia nigra. *Molecular Brain Research* **45**, 159–162 (1997).

57. Kemper, C. M., O'connor, D. T. & Westlund, K. N. Immunocytochemical localization of dopamine-β-hydroxylase in neurons of the human brain stem. *Neuroscience* **23**, 981–989 (1987).

58. Abercrombie, E. D. & DeBoer, P. Substantia Nigra D_1 Receptors and Stimulation of Striatal Cholinergic Interneurons by Dopamine: A Proposed Circuit Mechanism. *The Journal of Neuroscience* **17**, 8498–8505 (1997).

59. Espadas, I. *et al.* Dopamine D2R is Required for Hippocampal-dependent Memory and Plasticity at the CA3-CA1 Synapse. *Cerebral Cortex* **31**, 2187–2204 (2021).

60. Bannon, M. J. *et al.* Dopamine transporter mRNA content in human substantia nigra decreases precipitously with age. *Proceedings of the National Academy of Sciences* **89**, 7095–7099 (1992).

61. Nakamura, K., Ahmed, M., Barr, E., Leiden, J. M. & Kang, U. J. The Localization and Functional Contribution of Striatal Aromatic L-Amino Acid Decarboxylase to L-3,4-Dihydroxyphenylalanine Decarboxylation in Rodent Parkinsonian Models. *Cell Transplant* **9**, 567–576 (2000).

62. Shen, C.-H. Quantification and Analysis of Proteins. in *Diagnostic Molecular Biology* 187–214 (Elsevier, 2019). doi:10.1016/B978-0-12-802823-0.00008-0.

63. Bankhead, P. *et al.* QuPath: Open source software for digital pathology image analysis. *Sci Rep* **7**, 16878 (2017).

64. Hou, S. *et al.* Dopamine is produced in the rat spinal cord and regulates micturition reflex after spinal cord injury. *Exp Neurol* **285**, 136–146 (2016).

65. Li, Y. *et al.* Synthesis, transport, and metabolism of serotonin formed from exogenously applied 5-HTP after spinal cord injury in rats. *J Neurophysiol* **111**, 145–163 (2014).

66. Wienecke, J. *et al.* Spinal Cord Injury Enables Aromatic l-Amino Acid Decarboxylase Cells to Synthesize Monoamines. *The Journal of Neuroscience* **34**, 11984–12000 (2014).

67. Cassam, A. K., Llewellyn-Smith, I. J. & Weaver, L. C. Catecholamine enzymes and neuropeptides are expressed in fibres and somata in the intermediate gray matter in chronic spinal rats. *Neuroscience* **78**, 829–841 (1997).

68. Espana, R. A. Presynaptic dopamine modulation by stimulant self-administration. *Frontiers in Bioscience* **S5**, S371 (2013).

69. Ford, C. P. The role of D2-autoreceptors in regulating dopamine neuron activity and transmission. *Neuroscience* **282**, 13–22 (2014).

70. Li, Z. *et al.* Chronic Morphine Treatment Switches the Effect of Dopamine on Excitatory Synaptic Transmission from Inhibition to Excitation in Pyramidal Cells of the Basolateral Amygdala. *The Journal of Neuroscience* **31**, 17527–17536 (2011).

71. Lindgren, N. *et al.* Distinct roles of dopamine D2L and D2S receptor isoforms in the regulation of protein phosphorylation at presynaptic and postsynaptic sites. *Proceedings of the National Academy of Sciences* **100**, 4305–4309 (2003).

72. De Mei, C., Ramos, M., Iitaka, C. & Borrelli, E. Getting specialized: presynaptic and postsynaptic dopamine D2 receptors. *Curr Opin Pharmacol* **9**, 53–58 (2009).

73. Kim, J.-Y. V. *et al.* Spinal Dopaminergic Projections Control the Transition to Pathological Pain Plasticity via a D_1/D_5-Mediated Mechanism. *The Journal of Neuroscience* **35**, 6307–6317 (2015).

74. Morón, J. A., Brockington, A., Wise, R. A., Rocha, B. A. & Hope, B. T. Dopamine Uptake through the Norepinephrine Transporter in Brain Regions with Low Levels of the Dopamine Transporter: Evidence from Knock-Out Mouse Lines. *The Journal of Neuroscience* **22**, 389–395 (2002).

Appendix

Abstract

The catecholaminergic system plays a crucial role in modulating sensorimotor control in the spinal cord. Its proper function depends on catecholamines such as dopamine and noradrenaline, which are produced in supraspinal sources. Spinal cord injury (SCI) disrupts these descending catecholaminergic axonal projections, leading to axonal degeneration and impairing synaptic transmission in the spinal gray matter below the injury site. The aim of this study was to investigate for the first time the expression of key enzymes involved in catecholamine synthesis, including tyrosine hydroxylase (TH), aromatic L-amino acid decarboxylase (AADC) and dopamine β-hydroxylase (DBH), in human lumbar spinal cord tissue on protein level by immunohistochemistry and immunofluorescence. Additionally, AADC expression was also examined in human intact spinal cord tissue and in lumbar tissue after sustained SCI. Therefore, 4 intact spinal cords and 3 spinal cords with sustained SCI were included. The presence of the dopamine transporter (DAT) and the dopaminergic receptors D1 and D2 in the intact human lumbar spinal cord was investigated by using Western blot. TH, DBH and AADC were detected throughout the gray matter of the intact human lumbar spinal cord. The presence of DAT, D1 and D2 in the intact human lumbar spinal cord was confirmed by Western blot. A shift in AADC expression was observed in chronic SCI cases, characterized by increased expression in cell cytoplasms and a decreased immunopositivity on cell the dorsal horn, intermediate zone and ventral horn. These findings suggest a potential adaptive response in spinal gray matter to injury, possibly through increased local production of dopamine.

Zusammenfassung

Die katecholaminerge Neurotransmission spielt eine entscheidende Rolle bei der Modulation der sensomotorischen Kontrolle im Rückenmark. Dessen Funktion hängt von Katecholaminen wie Dopamin und Noradrenalin, die einensupraspinalen Ursprung aufweisen, ab. Eine Rückenmarksverletzung (SCI) unterbricht diese absteigenden katecholaminergen axonalen Projektionen und führt zu axonaler Degeneration sowie Beeinträchtigung der synaptischen Signalübermittlung im Rückenmark unterhalb der Läsionsstelle. Das Ziel dieser Studie war es, die Expression von Schlüsselenzymen, wie Tyrosinhydroxylase (TH), aromatische L-Aminosäure-Decarboxylase (AADC) und Dopamin-β-Hydroxylase (DBH), die an der Katecholaminsynthese beteiligt sind, erstmalig im humanen lumbalen Rückenmark auf Proteinebene mit Immunohistochemie und Immunofluoreszenz zu untersuchen. Darüber hinaus wurde die Expression von AADC in humanem lumbalen Rückenmark nach einer Querschnittsverletzung untersucht. Es wurden 4 Fälle mit intaktem Rückenmark und 3 Fälle mit einer Querschnittsverletzung inkludiert.Das Vorkommen des Dopamintransporters (DAT) und der Dopaminrezeptoren D1 und D2 wurde im intakten menschlichen Lumbalmark mittels Westernblot untersucht. TH, DBH und AADC wurden in der grauen Substanz des intakten menschlichen Lumbalmarks nachgewiesen. Das Vorhandensein von DAT, D1 und D2 im intakten menschlichen Lumbalmark wurde mittels Western Blot bestätigt. Bei chronischer Querschnittsverletzung wurde erhöhte Immunopositivität von AADC im Cytoplasma und eine geringere Expression an der Zellmembran im Hinterhorn, in der Intermediärzone und im Vorderhorn beobachtet. Diese Ergebnisse deuten auf eine potentielle adaptive Reaktion der grauen Substanz des Rückenmarks auf die Verletzung hin, welche möglicherweise auf eine erhöhte lokale Dopaminproduktion hinweist.